

Original Article

Identification of DHX36 as a tumour suppressor through modulating the activities of the stress-associated proteins and cyclin-dependent kinases in breast cancer

Yinduo Zeng^{1,2,3}, Tao Qin^{1,4}, Valentina Flamini², Cui Tan^{1,5}, Xinke Zhang⁶, Yizi Cong^{2,7}, Emily Birkin², Wen G Jiang², Herui Yao^{1,3}, Yuxin Cui²

¹Guangdong Provincial Key Laboratory of Malignant Tumour Epigenetics and Gene Regulation, Sun Yat-sen Memorial Hospital, Sun Yat-sen University, Guangzhou 510120, China; ²Cardiff China Medical Research Collaborative, Cardiff University School of Medicine, Heath Park, Cardiff CF14 4XN, UK; ³Breast Tumour Center, Sun Yat-sen Memorial Hospital of Sun Yat-sen University, Guangzhou 510120, China; ⁴Department of Medical Oncology, Sun Yat-sen Memorial Hospital of Sun Yat-sen University, Guangzhou, China; ⁵Department of Pathology, Sun Yat-sen Memorial Hospital of Sun Yat-sen University, Guangzhou, China; ⁶Sun Yat-sen University Cancer Centre, The State Key Laboratory of Oncology in South China, Collaborative Innovation Centre for Cancer Medicine, Guangzhou 510060, China; ⁷Department of Breast Surgery, The Affiliated Yantai Yuhuangding Hospital of Qingdao University, Yantai, China

Received September 25, 2020; Accepted November 29, 2020; Epub December 1, 2020; Published December 15, 2020

Abstract: The nucleic acid guanine-quadruplex structures (G4s) are involved in many aspects of cancer progression. The DEAH-box polypeptide 36 (DHX36) has been identified as a dominant nucleic acid helicase which targets and disrupts DNA and RNA G4s in an ATP-dependent manner. However, the actual role of DHX36 in breast cancer remains unknown. In this study, we observed that the gene expression of DHX36 was positively associated with patient survival in breast cancer. The abundance of DHX36 is also linked with pathologic conditions and the stage of breast cancer. By using the xenograft mouse model, we demonstrated that the stable knockdown of DHX36 via lentivirus in breast cancer cells significantly promoted tumour growth. We also found that, after the DHX36 knockdown (KD), the invasion of triple-negative breast cancer cells was enhanced. In addition, we found a significant increase in the number of cells in the S-phase and a reduction of apoptosis with the response to cisplatin. DHX36 KD also desensitized the cytotoxic cellular response to paclitaxel and cisplatin. Transcriptomic profiling analysis by RNA sequencing indicated that DHX36 altered gene expression profile through the upstream activation of TNF, IFN γ , NF κ B and TGF β 1. High throughput signalling analysis showed that one cluster of stress-associated kinase proteins including p53, ROCK1 and JNK were suppressed, while the mitotic checkpoint protein-serine kinases CDK1 and CDK2 were activated, as a consequence of the DHX36 knockdown. Our study reveals that DHX36 functions as a tumour suppressor and may be considered as a potential therapeutic target in breast cancer.

Keywords: DHX36, breast cancer, progression, stress-associated protein, CDK

Introduction

Breast carcinoma is one of the most common malignancies in women. Approximately 2.1 million new cases are diagnosed every year worldwide, which accounts for 25% of all the new female cancer cases, whereas 0.6 million deaths occur with a 5 year-survival range from 1-37% [1, 2]. The incidence, mortality rates and survival of breast cancer vary considerably, depending on complicated risk factors, subtype and stage. For instance, the triple-

negative breast cancer (TNBC) that is characterized by a lack of expression of estrogen receptor (ER), progesterone receptor (PR), or human epidermal growth factor receptor 2 (HER2), is the most aggressive subtype of breast cancer, with the highest rate of relapse and metastasis and the worst overall prognosis than other breast cancer subtypes. Hormone receptor-positive tumours like luminal A and luminal B can be treated with endocrine therapy, while a HER2-targeted therapy is usually used when HER2 is overexpressed. How-

ever, there is currently no targeted therapy available for TNBC, and chemotherapy is still the main treatment despite high frequencies of resistance. Therefore, novel biomarkers are needed for a more efficient treatment of some breast cancer subtypes such as TNBC.

DNA and RNA guanine-quadruplex structures (G4s) are often over-represented in gene promoter regions, regulatory regions of the human genome and untranslated regions of mRNAs. For example, G4s have been found in the gene promoters of proto-oncogenes including *MYC*, *KRAS*, *BCL-2* and *MLL*. The G4s are also enriched in the mRNAs of retinoblastoma protein 1 (*RB1*), *TP53*, vascular endothelial growth factor (*VEGF*), hypoxia-inducible factor 1 α (*HIF1 α), the transcription factor *MYB*, platelet-derived growth factor α polypeptide (*PDGFA*), PDGF receptor β polypeptide (*PDGFR β) and human telomerase reverse transcriptase (*TERT*). Therefore altered G4s have been implicated in cancer development and progression through mediating gene promoter activity or translation processes [3].**

Nucleic acid helicases are a large group of essential enzymes involved in a wide range of major DNA/RNA processing events, including DNA replication, RNA splicing, mRNA stability, ribosomal RNA maturation, microRNA processing, ribonucleoprotein (RNP) complex remodelling and RNA trafficking. The roles of some helicases (e.g. DDX1, DDX3, DDX5, DHX9, DDX41 and DDX43) in cancer have been well documented. For example, they can regulate tumorigenesis through the interaction with genes including *BRCA1*, *p53*, *c-Myc*, *Snail* and *E-cadherin*, and the modulation of some signalling pathways such as Wnt/ β -Catenin, L1TD1-RHA-LIN28 and NF- κ B signalling pathways [4, 5]. The DEAH-box polypeptide 36 (DHX36) was originally identified as a dominant ATP-dependent DEAH-box helicase highly specific for DNA and RNA G4s, and is also termed RNA helicase associated with AU-rich RNA element (RHAU) or G4 resolvase-1 (G4R1) [6].

DHX36 specifically binds and unwinds the G4-quadruplex motif with its ATPase and resolving activity. DHX36 has been considered as the major source of RNA G4-resolving activity in HeLa cell lysate. The depletion of DHX36 protein in HeLa cells causes a dramatic reduction in G4-DNA- and G4-RNA-resolving processes. DHX36 contributes to genomic integrity and

helps the transcription and the translation process by unwinding the secondary structures of certain nucleic acids. DHX36 also modulates some genes containing the G-quadruple forming regions, such as *p53*, *PITX*, *YY1*, *VEGF* and *ESR1* [7, 8]. For instance, DHX36 regulates *p53* pre-mRNA 3'-end processing following UV-induced DNA Damage. PITX1 protein acts as a tumour suppressor, and a reduction in its expression is associated with poor overall survival in lung cancer patients [9]. YY1 and VEGF proteins play a multifunctional regulatory role in breast cancer, while ESR1 is a predictor of clinical response to neoadjuvant hormonal therapy in breast cancer [10-12]. DHX36 can also interact with the pre-miR-134 terminal loop thus reducing the biosynthesis of miR-134 in neuronal dendrites [13]. Interestingly, miR-134 is implicated as a possible regulator in some cancer types and this may reinforce the role of DHX36 in tumours [14, 15]. It has also been reported that a long non-coding RNA gene G-Quadruplex Forming Sequence Containing lncRNA (GSEC) can antagonize DHX36 of its G-quadruplex unwinding activity which subsequently enhances the migration of colon cancer cells [16]. Despite the scattered findings above, the role of DHX36 in breast cancer has not been determined. Therefore, in this study, we aimed to investigate the functions of DHX36 in breast cancer cells and its carcinogenesis *in vivo*.

Materials and methods

Cell lines and culture conditions

All the breast cancer cell lines were purchased from the American Type Culture Collection (ATCC) and maintained at low passage (less than 20). Cells were cultured at 37°C in a humidified incubator supplied with 5% CO₂. The breast cancer cell lines were cultured in Dulbecco's modified Eagle's medium/F12K (Sigma-Aldrich, Dorset, UK) supplemented with 10% foetal calf serum (FCS, PAA Laboratories Ltd., Somerset, UK), penicillin (100 U/ml), and streptomycin (100 mg/ml) (Sigma-Aldrich).

Lentiviral infection with DHX36 shRNA

Lentiviral vectors containing short hairpin RNAs (shRNA) specific for DHX36 (namely, shRNA 1, shRNA 2 and shRNA 3) and the control shRNA (Scr control) were obtained from VectorBuilder (Santa Clara, CA, USA). The target sequences of the Scr controls and shRNAs were: Scr,

DEAH-box nucleic acid helicase DHX36 in breast cancer

CCTAAGGTTAAGTCGCCCTCG; shRNA 1, CCACGATCCAGGATGGATAT; shRNA 2, CCATAGATGATGTCGTTTATG; shRNA 3, CGATCTGACTTGAAAGTAATA. The vectors were assembled with EGFP as a reporter and neomycin resistant gene for selection. HEK293T packaging cells were transduced with viral packaging (pSPAX2), viral envelope (pMD2G) and lentiviral plasmid vectors using FuGENE 6 transfection reagent (Promega, Southampton, UK) in serum-free OPTI-MEM (Invitrogen, Carlsbad, CA, USA). Four and five days after transfection, the supernatant containing the packaged viral particles was collected and filtered through a 0.45 µm filter. MDA-MB-231 and BT549 breast cancer cells were then infected using the lentiviral supernatant in the presence of 8 µg/ml Polybrene (Sigma-Aldrich). After 48 hours, the cells were selected with 1.2 mg/ml G418 for 7 days, and maintained in a growth medium with 300 µg/ml G418. After selection, the stable breast cancer cell lines spontaneously expressed GFP which could be visualized under a fluorescence microscope.

Drug cytotoxicity assay

Breast cancer cells at a density of 8000 cells/well were seeded into 96-well plates and starved using a medium containing 2% FCS. Cells were then treated with a serial dilution of cisplatin (Tocris Cookson Ltd., Bristol, UK), paclitaxel (Tocris) and flavopiridol (Cambridge Bioscience, Cambridge, UK), respectively. The vehicle control of cisplatin was ddH₂O, while the vehicle control of paclitaxel and flavopiridol was DMSO. After treatment for 24 and 48 hours, the cells were stained with Alamar Blue (Bio-Rad, Cambridge, MA, USA) following the manufacturer's instruction. The fluorescence was read with an excitation wavelength of 530 nm and the emission at 590 nm using a Glomax Multi Detection System (Promega).

To analyse the basal proliferation levels of the stable breast cancer cell lines in the absence of any drug treatment, cells were seeded at two densities (2500 and 5000 cells/well) in 96-well tissue-culture plates, and measured using the method as above after cultivation for three time points (0, 24 and 48 hours).

Cell-matrix adhesion assay

Tissue culture plates (96-well black-well) were pre-coated with 3 mg/ml of Matrigel Matrix in

serum-free medium (BD Biosciences, San Diego, CA, USA) and left overnight at 37°C. Cells at a density of 10,000 cells/well were seeded onto the pre-coated plates. Following incubation for 1 hour, the non-adherent cells were washed off with PBS. The adherent cells were stained with 1 µM of Calcein AM (eBioscience, Hatfield, UK) for 30 minutes at 37°C. The fluorescence, which is proportional to the number of the adhesive cells, was read with an excitation wavelength of 485 nm and the emission at 520 nm using a Glomax Multi Detection System (Promega Wisconsin USA).

Electric cell-substrate impedance sensing (ECIS)

The migration ability of breast cancer cell lines was monitored using the ECIS system. Briefly, MDA-MB-231 and BT549 cells at a density of 2.5×10^4 cell/well were seeded onto ECIS 96W1E array plates (Applied Biophysics Inc. NY, USA). The electrical resistance, due to the interaction of cells and gold-coated electrodes, was recorded. Once a confluent monolayer was formed, the cells were subjected to an electric wound at 2800 µA, 60 kHz for 20 seconds and the rate of change in impedance, as cells migrated onto the electrode sensing area, was subsequently monitored and analysed.

Transwell invasion assay

The membrane of 24-well inserts with an 8 µm pore size (Greiner Bio-one, Frickenhausen, Germany) was pre-coated with 300 µg/ml of Matrigel for 2 hours at 37°C. 1×10^5 cells were then seeded onto the top chamber in 400 µl of serum-free medium, and 600 µl of the same medium containing 10% FCS was added to the lower chamber. After incubation for 24 hours, the invaded cells were detached with 400 µl of HyQase Dissociation solution (HyClone, Logan, UT, USA) and stained with 1 µM calcein-AM for 1 h. The cell solution was then transferred to a 96-well black-well plate at a volume of 100 µl/well for 3 wells per group. The fluorescence of invaded cells was measured using the Glomax Multi Detection System.

Western blotting

Cultured cells were washed twice in PBS and lysed in RIPA buffer containing 50 mM Tris-HCl, 2% SDS, 5% glycerol, 5 mM EDTA, 1 mM NaF, 10 mM β-glycerophosphate, 1 mM PMSF,

1 mM Na₃VO₄ and EDTA-free Protease Inhibitor Cocktail (Roche, Mannheim, Germany). Protein concentration was determined by the Pierce BCA protein assay (Thermo Scientific, Colchester, UK). After normalization, proteins were separated by sodium dodecyl sulphate-polyacrylamide gel electrophoresis (SDS-PAGE) and transferred with a semi-dry fast transfer apparatus onto a PVDF membrane (Merck Millipore Inc., Billerica, USA). The membranes were blocked with 5% non-fat dried milk (Marvel, Premier Beverages, Stafford, UK) in PBST solution (0.05% Tween-20 in PBS) for 1 h at room temperature. The membranes were then incubated with the primary antibodies diluted in 5% milk and left overnight at 4°C. Following three washes with PBST, the membranes were incubated with a diluted HRP-conjugated secondary antibody for 1 h at room temperature. The primary antibodies were anti-JNK (diluted 1:1000. Sc-571, Santa Cruz Biotechnology, Santa Cruz, CA, USA), anti-pJNK^{Thr 183/Tyr 185} (diluted 1:1000. sc-6254, Santa Cruz), DHX36 (diluted 1:1000. GTX-131179, GeneTex, San Antonio, TX, USA) and β-actin (diluted 1:5000. sc-53142, Santa Cruz). The HRP-secondary antibodies (A5278, Anti-Mouse IgG; A0545, Anti-Rabbit IgG) were diluted at 1:2000 (Sigma-Aldrich, Dorset, UK). Protein detection was performed using an EZ-ECL chemiluminescence kit (Biological Industries USA, Inc., Cromwell, CT, USA). Immunoreactive bands were visualized and quantified by densitometry using the Syngene G:BOX chemiluminescence imaging system and Gene Tools 4.03 (Syngene Europe, Cambridge, UK).

Reverse transcription (RT) and real-time PCR analysis

RNA was extracted from the cultured cells at the 60-80% confluency in T25 flasks using TRI Reagent (Sigma-Aldrich, Dorset, UK). Total RNA (500 ng) was reverse-transcribed to complementary DNA (cDNA) using Goscript Reverse Transcription mix (Promega). Following dilution of cDNA at a ratio of 1:8, the quantitative real-time PCR was performed based on an Amplifluor™ technology, in which a 6-carboxy-fluorescein-tagged Uniprimer™ (Biosearch Technologies, Inc., Petaluma, CA, USA) was used as a probe along with a pair of specific primers with an addition of a Z-sequence (act-gaacctgaccgtaca) to the 5'-end of the reverse

primer [17]. The primer sequences for qPCR were: DHX36 forward primer, GTTTAAATCAGTTAACCAGACAC; DHX36 reverse primer, ACTGAACCTGACCGTACACGCAATGTTGGTAGCAATTA; JNK forward primer, CTACAAGGAAAACGTTGACA; JNK reverse primer, ACTGAACCTGACCGTACAGAACAAAACACCACCTTTGA; β-actin forward primer, CATTAAAGGAGAAGCTGTGCT; β-actin reverse primer, ACTGAACCTGACCGTACAGCTCGTAGCTCTTCTCCAG. The qPCR assays were run in a StepOnePlus system (Thermo Fisher Scientific, Waltham, MA, USA) and normalized by the corresponding threshold cycle (CT) values of β-actin mRNA.

Xenograft tumour model

BALB/c female nude mice (6-8-week old) were purchased from Beijing Vital River Laboratory Animal Technology Co., Ltd. (Beijing 100107, China) and bred in a specific pathogen-free (SPF) animal house at approximately 28°C in an environment with approximately 50% humidity. They were randomly assigned to two groups with 10 mice/group. 3 × 10⁶ of stable MDA-MB-231 cell lines containing either Scr control or DHX36 shRNA were harvested, resuspended in 0.1 mL of PBS, and subcutaneously transplanted into mammary fat pads of the allocated mice. Each mouse received one injection. The Tumour size was measured with a calliper every 3-4 days and calculated in mm³ using the formula for a prolate spheroid (width² × length × 0.523). When the tumour mass reached the maximum allowed size (16 mm in diameter), the mice were imaged using an IVIS imaging system (Perkin Elmer, Santa Clara, CA, USA) following the manufacturer's instruction. The mice were then sacrificed and the tumours were excised, photographed and weighed. The freshly dissected tumours were fixed in 10% formalin overnight and embedded in paraffin. All the animal experiments were approved by the Institutional Animal Care and Use Committee of Sun Yat-sen University Cancer Centre.

Immunohistochemistry (IHC) of tissue microarray

The breast cancer tissue microarrays were purchased from US Biomax Inc. (BR1921b, HBre-Duc140Sur-01 and BR1503e. Rockville, MD, USA). The standard indirect biotin-avidin immunohistochemical analysis was used to evalu-

ate the DHX36 protein expression. Briefly, the microarray slides were placed in an oven at 50°C for 1 day to facilitate the adhesion of tissue sections to the slides. The tissue microarrays were then dewaxed and rehydrated by sequential treatment (5 min per step) with xylene, xylene/ethanol, a serial dilution of ethanol (100%, 90%, 70%, 50%), distilled H₂O and Tris-buffered saline (TBS) buffer. Antigen retrieval was performed by placing the slides in a plastic container, covered with 0.01 M sodium citrate buffer (pH 6.0) antigen retrieval buffer, and heated in a microwave on full power for 20 minutes. Endogenous peroxide activity was blocked by incubating the sections with 3% hydrogen peroxide for 10 minutes. After 1 hour of pre-incubation in 5% normal goat serum to block nonspecific staining, the sections were incubated with 7.5 µg/ml of the DHX36 antibody (GTX131179, GeneTex) overnight at 4°C. The slides were then washed four times with TBS, and incubated with a universal biotinylated secondary antibody (ABC Elite Kit, Vectastain Universal, PK-6200, Vector Laboratories, CA, USA) for 30 minutes. Following washing with TBS, the sections were incubated with avidin-biotin-peroxidase complex (ABC) for 30 minutes. The 3, 3'-diaminobenzidine (DAB) substrate (5 mg/ml) was used to develop the final reaction product. The sections were then rinsed in water, counterstained with Gill's hematoxylin (Vector Laboratories), and dehydrated through a series of graded alcohols, cleared in xylene and mounted in DPX/Histomount (Merck Millipore, UK). Images were captured using an EVOS FL Auto 2 Cell Imaging System (ThermoFisher Scientific). All IHC images were manually evaluated and scored by two pathologists independently who were blinded to the clinical information. The immunohistochemical score was calculated based on intensity plus the percentage of tumour staining. The cut-off value was set as an upper quarter of the score divided into a high and low expression of DHX36 protein.

Flow cytometry

Cultured cells were detached with trypsin/EDTA and fixed with the IC fixation buffer (ThermoFisher Scientific) for 1 h at room temperature, then resuspended in ice-cold 100% methanol, and incubated overnight at -20°C. Cells were then washed twice in FACS buffer (2 mM EDTA in PBS, pH 7.4), blocked with 1%

bovine serum albumin (BSA) in PBS with 0.1% Tween for 1 hour. For the staining with antibodies, cells were incubated with diluted primary antibodies (1:100) including normal mouse IgG (14-4714-82, ThermoFisher Scientific), cleaved poly (ADP-ribose) polymerase (PARP) (14-6668-82, ThermoFisher Scientific), JNK and p-JNK, respectively, for 1 hour at room temperature. Cells were then incubated with Alexa Fluor 647-conjugated goat anti-mouse IgG antibodies (1:1000; A21235, ThermoFisher Scientific) for 30 minutes at room temperature. For cell cycle analysis, cells were harvested and blocked as described above, and then directly incubated with Hoechst 33342 (10 µg/ml, H3570, ThermoFisher Scientific) for 1 hour at 37°C in the dark. Following the final wash with FACS buffer, FACS was performed using BD FACS Canto II flow cytometer equipped with FACS Diva Software (version 6.1.2, BD Biosciences, San Jose, CA, USA). FACS data were analysed using FCS Express software (version 4, De Novo Software, Los Angeles, CA, USA).

Bioinformatic analysis of gene expression and survival

The association between DHX36 gene expression and the survival of breast cancer patients was assessed using the pooled gene expression data from www.kmplot.com. The online tool allowed us to analyse both the OS (overall survival) and RFS (relapse-free survival) from 626 cases of breast cancer and the RFS from 1764 cases which were subjected to expression profiling with Affymetrix GeneChip microarray (DHX36 Probeset ID: 223140_s_at). The Auto select best cutoff was chosen. The differential expression of DHX36 was examined by a pooled analysis of The Cancer Genome Atlas-Breast invasive carcinoma (TCGA-BRCA) dataset which contains 1097 breast-cancer patients and 114 normal samples.

RNA sequencing (RNA-Seq)

The global transcriptomic profiling was analysed by RNA-Seq on the BGISEQ-500RS sequencer (BGI, Shenzhen, China) which generated 50-bp paired-end reads. The statistical enrichment and molecular network of differentially expressed genes (DEGs) were analysed using the Ingenuity Pathway Analysis (IPA) software (Qiagen, Germany).

Kinexus Kinex antibody microarray

The stable breast cancer cell lines were seeded in T75 flasks and incubated in DMEM supplemented with 10% FCS at 37°C. When the confluence was approximately 80%, the cells were then washed twice, and the culture medium was replaced with DMEM with 2% FCS. After incubation overnight, cells were suspended in lysis buffer, pH 7.4, containing 100 mM Tris Buffer, 10% 2-ME, 1% NP-40, protease inhibitor cocktail tablet and 50 mM NaF. The lysates were vortexed and homogenized on a blood wheel for 1 hour at 4°C. The supernatant of the lysates was then collected by centrifugation for 30 minutes at 15,000 rpm at 4°C, the protein concentration in the supernatant was determined by a fluorescamine protein quantification assay (Sigma-Aldrich). Proteomic analysis of pan-specific and phosphorylated proteins was carried out using a high throughput Kinex antibody microarrays (900 antibodies, Kinexus Bioinformatics) (<http://www.kinexus.ca/services>).

Statistical analysis

For quantitative measurement, including cell-based assays and gene expression profiling, the Shapiro-Wilk test was used to verify whether the data were normally distributed. For the comparison of the difference from two subjects, an unpaired t-test was used for data with normal distribution, whereas, for non-normal distribution, the Mann-Whitney Rank Test was applied. When more than two sets of data were compared, either One-Way ANOVA or the non-parametric Kruskal-Wallis test was used. Pearson chi-square test was used to test the association of the categorized scoring data from tissue microarray IHC staining and clinical features. Graphs and the statistical analysis were performed using R (version 3.6.1, <https://www.r-project.org>) or GraphPad Prism 8 software (GraphPad Software, San Diego, CA, USA). Statistical significance was indicated with the following nomenclature: *P<0.05, **P<0.01, ***P<0.001 unless the p-values were shown.

Results

Lower gene expression of DHX36 is associated with poorer survival

We assessed the prognostic value of DHX36 gene expression in breast cancer using the

Kaplan-Meier plotter containing 1764 samples from breast cancer patients. As shown in **Figure 1A** and **1B**, lower expression of DHX36 mRNA correlated with poorer OS (HR=0.63 (0.45-0.88). P=0.0059) and RFS (HR=1.32 (1.13-1.54). P=0.023) when all the types of breast cancer were pooled together. We then analysed the differential expression of the DHX36 gene in the database of the TCGA invasive breast carcinoma (TCGA-BRCA). It showed that there is a lower level of DHX36 gene expression in primary tumour compared to normal tissue control (P=0.0092; **Figure 1C**). The DHX36 gene expression was down-regulated in the later stages (T3+T4) of the breast carcinoma compared to the earlier stages (T1+T2) (P=0.0096, **Figure 1D**). Also, it appeared that the gene expression level of DHX36 was higher in TNBC (n=123) than in non-TNBC (n=605) (P<0.0001, **Figure 1E**).

Low level of the DHX36 protein also predicts poor survival as indicated by tissue microarray IHC

We then estimated the IHC staining of the DHX36 protein in breast cancer tissue microarrays from patient specimens. As shown in **Table 1** and **Figure 1F, 1G**, the samples from patients at a higher stage (2 & 3) showed weaker staining of DHX36 (score 0 & 1) (P=0.034 than lower stage). When we compared the different pathological types, the frequency of the lower stained DHX36 was higher in IDC (214/277=77.26%) than in ILC (3/81=3.70%) and in adjacent normal tissue (9/34=26.47%) (P<0.001). The expression level of the DHX36 protein also appeared to be associated with the pathological diagnosis (P<0.001), HER2 intensity (P<0.001), ER intensity (P<0.001) and PR intensity (P<0.001). We then performed a Kaplan-Meier survival analysis using a dataset of one array with definite follow-up status (n=140, #HBre-Duc140Sur-01). A higher level of DHX36 protein expression correlated with favourable survival of breast cancer patients (**Figure 1H**). The thumbnail IHC images of the three tissue microarrays are shown in Supporting Information [Figure S1](#).

Knockdown of DHX36 in TNBC cells increased the invasion ability and suppressed the migration of the tumour cells in vitro

To understand the role of DHX36 in breast cancer, we selected two TNBC cell lines for a

DEAH-box nucleic acid helicase DHX36 in breast cancer

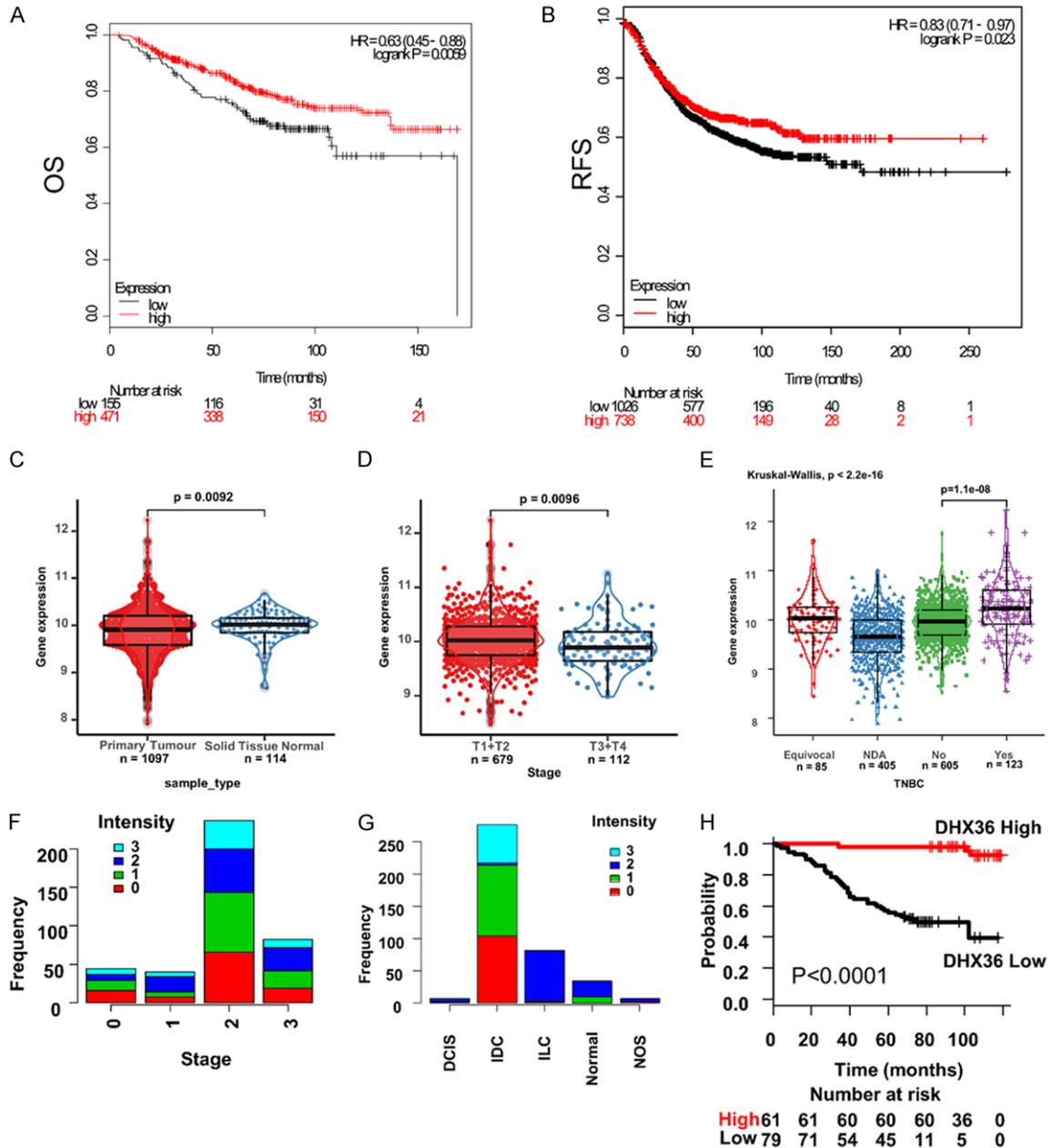


Figure 1. Expression levels of DHX36 gene and protein are associated with the survival and clinicopathological features of breast cancer patients. The Kaplan-Meier survival curve was plotted using the pooled gene expression data from www.kmplot.com (Cut-off value: 1257.33, n=1764). A. OS. B. RFS. C. DHX36 gene expression is down-regulated in the primary tumour as indicated by the analysis of The Cancer Genome Atlas-Breast invasive carcinoma (TCGA-BRCA) dataset (n=1211). D. Expression level of the DHX36 gene is lower in advanced stages (T3+T4) than in earlier stages (T1+T2) as indicated by the TCGA-BRCA data. E. Expression level of the DHX36 gene is higher in TNBC (n=123) than in non-TNBC (n=605) as indicated by the TCGA-BRCA data. Equivocal: The ER/PR/HER3 status is partially determined. NDA: No data available for the ER/PR/HER3 status. F. Frequency of DHX36 staining scores in different pathological types in breast cancer tissue arrays. G. Frequency of DHX36 staining scores in different stages in breast cancer tissue arrays. H. Kaplan-Meier survival analysis of the breast cancer tissue arrays following DHX36 staining by immunohistochemistry. Representative images of the differential staining intensity of DHX36 in normal breast and breast cancer tissues were shown in Supporting Information [Figure S1](#). Clinicopathological status of the three tissue microarray slides was provided in [Table 1](#).

stable DHX36 knockdown after initial evaluation of the gene and protein expression levels

of DHX36 in a panel of breast cancer cells (Supporting Information [Figure S2](#)). As shown in

DEAH-box nucleic acid helicase DHX36 in breast cancer

Table 1. The association of the IHC staining intensity of DHX36 and clinical features of breast cancer patients

Clinical feature	DHX36 intensity				P-value (chi-square test)
	0	1	2	3	
Pathological diagnosis					
Adjacent normal	13	6	5	7	
Cystosarcoma phyllodes	0	2	0	0	
DCIS	0	0	0	1	
Fibroadenoma	0	3	0	0	
Intraductal carcinoma	0	3	1	1	
Intraductal carcinoma (sparse)	0	1	0	0	
Intraductal carcinoma with early infiltrate	0	0	1	0	
IDC	34	82	89	48	
IDC (sparse)	0	0	1	0	
IDC and ILC	0	1	0	0	
IDC with ILC	0	0	3	0	
IDC with micropapillary carcinoma	0	1	6	2	
IDC with mucinous carcinoma	0	0	2	2	
IDC with necrosis	0	0	1	1	
IDC (blank)	0	1	0	0	
IDC (sparse)	1	0	0	0	
ILC	55	21	4	0	
ILC (blank)	2	0	0	0	
Mucinous carcinoma	0	0	2	0	
Normal breast tissue	1	0	0	0	
Normal breast tissue (fibrous tissue)	2	0	0	0	1.582E-15
Stage					
1	7	7	20	6	
2	66	77	57	37	
3	19	23	29	11	0.03446
HER2 intensity					
Unknown	9	1	1	5	
0	79	30	15	12	
1	3	52	6	2	
2	3	11	4	0	
3	11	17	3	2	2.016E-15
ER intensity					
Unknown	9	2	2	5	
0	19	61	16	6	
1	16	11	4	2	
2	17	14	1	2	
3	44	22	6	6	1.544E-06
PR intensity					
Unknown	8	2	3	4	
0	30	75	15	8	
1	22	10	2	2	
2	17	12	3	1	
3	28	11	6	6	6.486E-06
Pathology					

DEAH-box nucleic acid helicase DHX36 in breast cancer

DCIS	1	0	4	2	
IDC	104	110	3	60	
ILC	1	2	78	0	
Normal	0	9	25	0	
NOS	2	0	5	0	2.20E-16

DCIS: ductal carcinoma in situ. IDC: invasive ductal carcinoma. ILC: invasive lobular carcinoma. NOS: not otherwise specified.

Figure 2, after the establishment of the stable knockdown cell lines using BT549, all three shRNAs (1, 2 and 3) reduced the gene expression of DHX36 when compared with scramble (Scr) shRNA and wild-type (WT) controls (**Figure 2A**). Likewise, this was also the case in the stable cell lines developed from MDA-MB-231 (**Figure 2B**). The Western blotting images also showed that in BT549, the DHX36 protein level was dramatically reduced in all three cell subsets (shRNA 1, 2 and 3) with the shRNA 2 showing the best efficiency (**Figure 2C**). As expected, the WT and Scr controls showed a higher expression of DHX36 protein. The efficiency of shRNA 2 was subsequently demonstrated in the stable cell lines developed from MDA-MB-231.

We then evaluated the effect of DHX36 expression on tumour cell invasion using the Matrigel-coated transwell chamber. As shown in **Figure 2E**, in BT549 cells, DHX36 shRNA 2 increased the invasion by 6.39% compared to the Scr control ($P < 0.0001$). Similarly, in MDA-MB-231 cells, DHX36 shRNA 2 increased the invasion by 10.83% compared to the Scr control ($P = 0.041$, **Figure 2F**).

To assess whether the effect of ShRNA 2 on breast cancer cells were mainly due to the off-target effect, we repeated the invasion assay using both shRNA 1 and shRNA 2. The result showed that in the cell lines established from BT549, both shRNA 1 and shRNA 2 promoted the tumour cell invasion significantly ($P < 0.01$). In the cell lines established from MDA-MB-231, the knockdown of DHX36 by the two shRNAs also promoted the cell invasion ($P < 0.01$), and the effect of shRNA 1 appeared stronger than shRNA 2. These repeated data therefore not only suggested that the effect is unlikely the off-target effect of shRNA 2 but also confirmed that the effect of DHX36 on breast cancer cell invasion was reproducible (Supporting Information [Figure S3](#)). Because shRNA 2 is the most potent one, therefore, in the following experiments, only the stable cell lines with shRNA 2 were utilised (named as shRNA unless otherwise described).

We monitored the cell migration using the ECIS system and found that DHX36 shRNA inhibited the migration of the breast cancer cells after the electric wound ($P < 0.01$ vs. Scr control, respectively. **Figure 2G, 2H**).

Knockdown of DHX36 in TNBC cells increases the S-phase cell population and de-sensitize the apoptotic response to cisplatin

We investigated the role of DHX36 in the cell cycle by flow cytometry. As shown in **Figure 3A-D**, DHX36 knockdown in the BT549 stable cell lines increased the S-phase population to 36.23% from 25.91% (Scr). Similarly, in the MDA-MB-231 stable cell line, the DHX36 knockdown increased the S-phase cell population to 43.65% from 33.37% (Scr). We then analysed the intrinsic proliferation levels of the stable cells to evaluate whether the increase of S-phase in the cell cycle by the knockdown of DHX36 affects the change of proliferation. The result indicated that in the BT549 stable cell lines, from both cell density settings, there was no significance after cultivation for 24 and 48 hours. In the cell lines established from MDA-MB-231, from the seeding density of 2500 cells/well, shRNA 2 increased the proliferation level mildly at Hour 48 ($P < 0.05$); and from the seeding density of 5000 cells/well, the increase in proliferation by shRNA can be observed at Hours 24 and 48, respectively ($P < 0.01$) (Supporting Information [Figure S4](#)). The proliferation data therefore suggest the role of DHX36 in the growth of breast cancer cells may be either cell-dependent or limited.

We then evaluated the effect of DHX36 knockdown on apoptosis of the breast cancer cells using the cleaved PARP as an indicator. In the BT549 stable cell lines, the knockdown of DHX36 decreased the basal apoptotic level by approximately 19.96% compared to its Scr control (**Figure 3E, 3F**); cisplatin (16 μ M, 24 hours) increased the apoptosis of the Scr control by approximately 45.14%, but just increas-

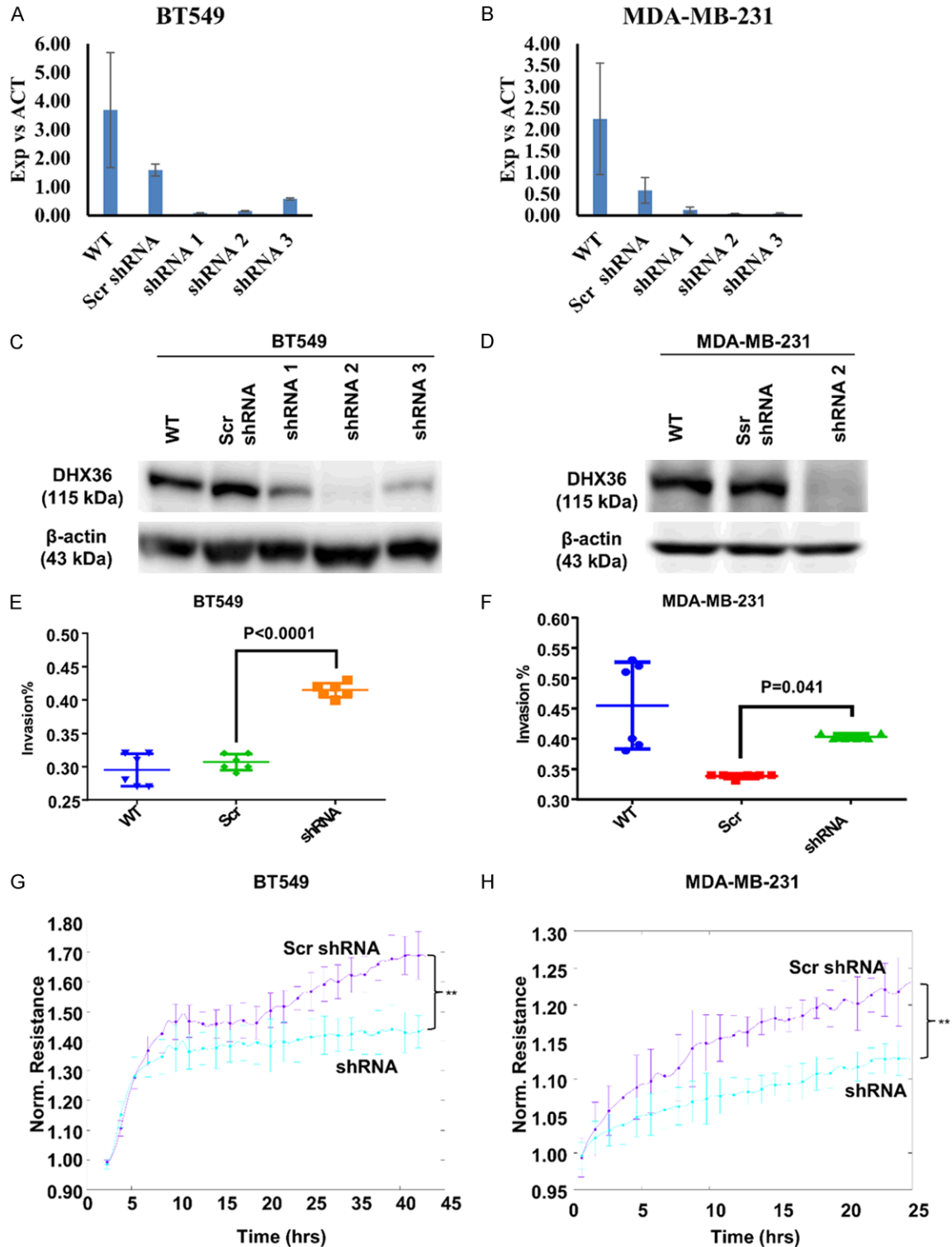


Figure 2. Knockdown of DHX36 enhanced invasion but decreased migration of breast cancer cells. A. Relative gene expression of DHX36 in BT549 cells following DHX36 knockdown with shRNA. B. Relative gene expression of DHX36 in MDA-MB-231 cells following DHX36 knockdown with shRNA. C. The expression level of DHX36 protein after stable shRNA knockdown of DHX36 in BT549 cells, as estimated by Western blotting. D. The expression level of DHX36 protein after stable shRNA knockdown of DHX36 in MDA-MB-231 cells, as estimated by Western blotting. E, F. Transwell invasion assay using the stable cell lines derived from BT549 and MDA-MB-231 cells, respectively. Cells invaded through Matrigel-coated membrane inserts (pore size 8 μ m) were stained with Calcein AM and detached using Cell Dissociation Solution, and read using a fluorescence plate reader. The cell group with DHX36 shRNA was

DEAH-box nucleic acid helicase DHX36 in breast cancer

compared with the Scr Control. Although the Invasion of the WT control was showed, because WT cells were not subjected to lentiviral infection and specific G418 selection, they were not directly comparable to the shRNA groups. Student T-tests were used to compare the difference between shRNA and Scr. G, H. Effect of DHX36 knockdown on the migration of breast cancer cells was accessed using the electric cell-substrate impedance sensing system (ECIS). Normalization was performed by setting up the stating impedance signal for each group to 1. The repeated-measures ANOVA was used to compare the ECIS data from different cell groups. **P<0.01.

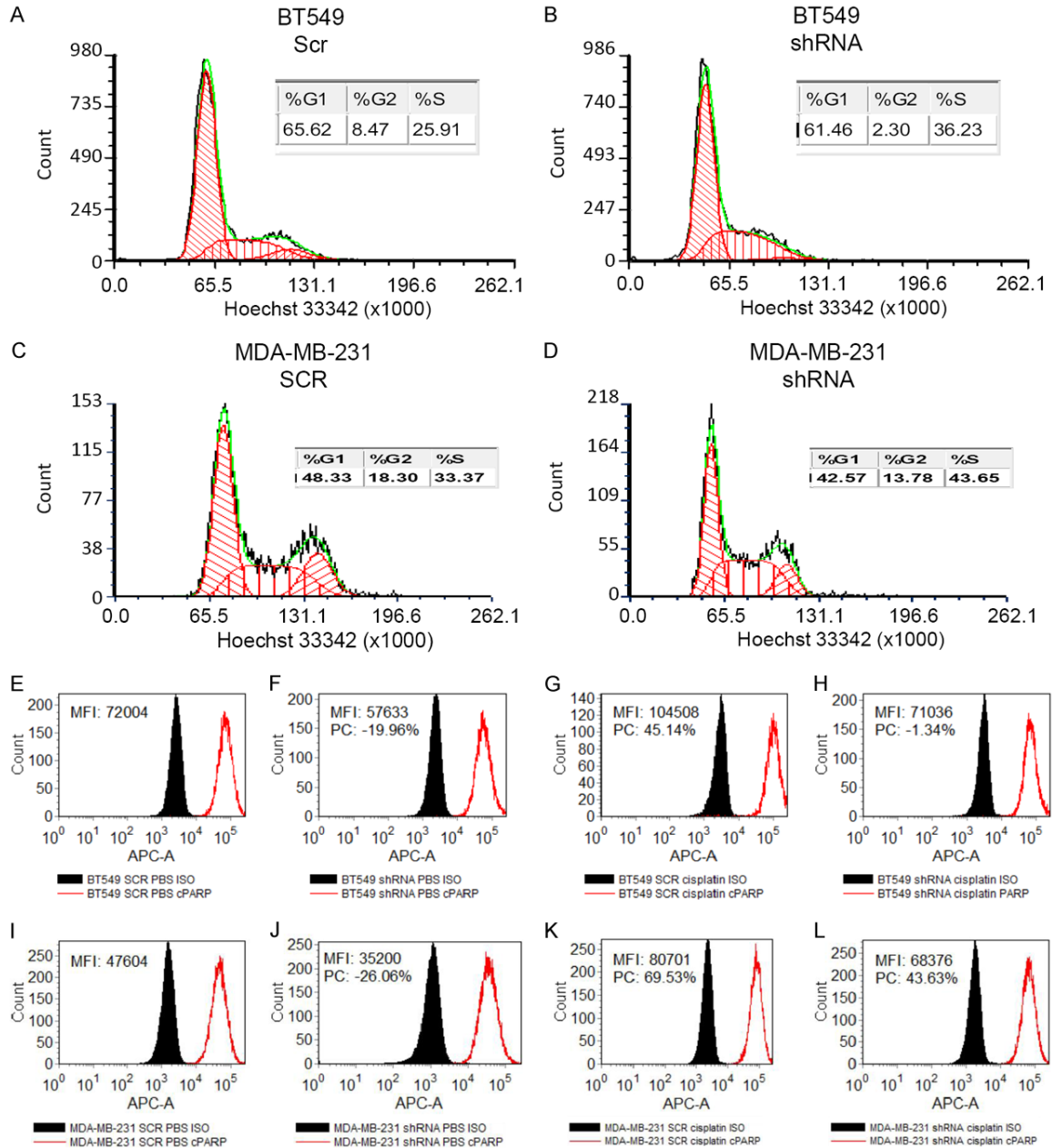


Figure 3. Effect of DHX36 knockdown on cell cycle progression and apoptosis in response to cisplatin. Hoechst 33342 was used to stain cellular DNA for cell cycle profiling, while the apoptosis level was determined using a cleaved-PARP (cPARP) antibody. A, B. Cell cycle analysis of BT549 cells transduced with Scr control (left) and DHX36 shRNA (right). C, D. Cell cycle analysis of MDA-MB-231 cells transduced with Scr control (left) and DHX36 shRNA (right). E-H. Level of cleaved-PARP in BT549 cells transduced with Scr control and DHX36 shRNA, and treated with PBS and cisplatin, respectively. I-L. Level of cleaved-PARP in MDA-MB-231 cells transduced with Scr control and DHX36 shRNA, and treated with PBS and cisplatin, respectively. The levels of the cleaved-PARP were indicated using the Median Fluorescence Intensity (MFI). The percentage change of MFI (PC) was calculated using the equation: $PC = (MFI_{test} - MFI_{control}) / MFI_{control} * 100$, where control means the Scr PBS group. ISO, isotype control.

ed the apoptosis of the DHX36 knockdown group by approximately 18.62% in comparison to its vehicle (PBS) control (**Figure 3G, 3H**). In the MDA-MB-231 stable cell lines, the knockdown of DHX36 decreased the basal apoptotic level by approximately 26.06% compared to its Scr control (**Figure 3I, 3J**); cisplatin increased the apoptosis of the Scr control by approximately 69.53%, and increased the apoptosis of the DHX36 knockdown group by approximately 69.69% in comparison to its vehicle (PBS) control (**Figure 3K, 3L**). The data, therefore, suggest that DHX36 may modulate the intrinsic apoptosis of breast cancer cells. And it appeared that cisplatin raised a stronger apoptotic response in MDA-MB-231 cells than BT549 cells.

Knockdown of DHX36 desensitizes the susceptibility of breast cancer cells to chemotherapeutic drugs in a cell- and dose-dependent manner

We then evaluated the cytotoxic response of breast cancer cells to some chemotherapeutic drugs including paclitaxel and cisplatin. As shown in **Figure 4A**, in MDA-MB-231 cells, following 24-hour treatment, the decrease of cell viability started to be observed from 5 nM paclitaxel in the Scr group, while the DHX36 knockdown group showed the viability decrease from 10 nM. The suppression of the cellular susceptibility to paclitaxel by DHX36 knockdown can be seen from 5 nM to 40 nM in comparison to the Scr controls ($P < 0.01$ vs. Scr, respectively). The response difference between the two stable MDA-MB-231 cell lines to paclitaxel began to disappear following treatment for 48 hours (**Figure 4B**). Similarly, the lower level of cytotoxic response to paclitaxel was observed in the DHX36-knockdown BT549 cell line compared to the Scr control after treatment for 24 hours (**Figure 4C**). Again, the response difference of the two stable BT549 cell lines to paclitaxel began to disappear following treatment for 48 hours (**Figure 4D**). Independent to the effect of DHX36 knockdown, we noticed that the control BT549 cell line was more sensitive to paclitaxel (starting from 2.5 nM) compared to the control MDA-MB-231 cell line (starting from 5 nM). Following treatment with multiple doses of cisplatin for 24 hours, the DHX36-knockdown MDA-MB-231 cell line showed a higher proliferation ratio,

thus lower cytotoxicity, in response to the doses of 32 μM ($P < 0.05$) and 64 μM ($P < 0.01$) than the Scr control (**Figure 4E**). The response significance of the two stable MDA-MB-231 cell lines to cisplatin was observed to sustain following treatment for 48 hours ($P < 0.01$ for the two high working doses) (**Figure 4F**). Likewise, In BT549 cells, DHX36 knockdown also led to a reduction of the cellular response to cisplatin following treatment for 24 and 48 hours (**Figure 4G, 4H**). We also confirmed that the control BT549 cell line was more sensitive to cisplatin (starting from 1 μM) compared to the control MDA-MB-231 cell line (starting from 4 μM).

Knockdown of DHX36 promotes breast cancer development in a mouse xenograft

To examine whether the DHX36 knockdown promotes breast cancer growth *in vivo*, we inoculated the stable MDA-MB-231 cells with and without DHX36 knockdown in nude mice. The *in-vivo* fluorescence imaging analysis indicated that all the nude mice showed some tumour growth after implantation with the stable cell lines containing either the Scr control (**Figure 5A**) or the DHX36 shRNA (**Figure 5B**). The tumours with bigger sizes could be visualized from the group of the DHX36 shRNA. The quantification of individual tumour fluorescence images confirmed that the mice group of the DHX36 shRNA had larger total tumour pixels (proportional to tumour size) compared to the Scr control ($P < 0.01$, **Figure 5C**). Likewise, the mice group of the DHX36 shRNA showed a higher level of the integrated density of tumour fluorescence (proportional to tumour mass density) compared to the Scr control ($P < 0.05$, **Figure 5D**). The data of the time-lapse physical measurement of the xenograft mice indicated that the mice with the DHX36 knockdown started to develop a bigger tumour mass (average tumour volume in mm^3) than the Scr control after 2 weeks. This trend of accelerated tumour growth continued until the end of examination at Day 46 ($P < 0.001$, **Figure 5E**). No significant change of body weight was observed between the two mice groups over the course of the measurement ($P > 0.05$, **Figure 5F**). The dissected tumours from the mice group containing the DHX36 knockdown cells at the endpoint (Day 46) presented larger tumours (**Figure 5G**). The measurement of the

DEAH-box nucleic acid helicase DHX36 in breast cancer

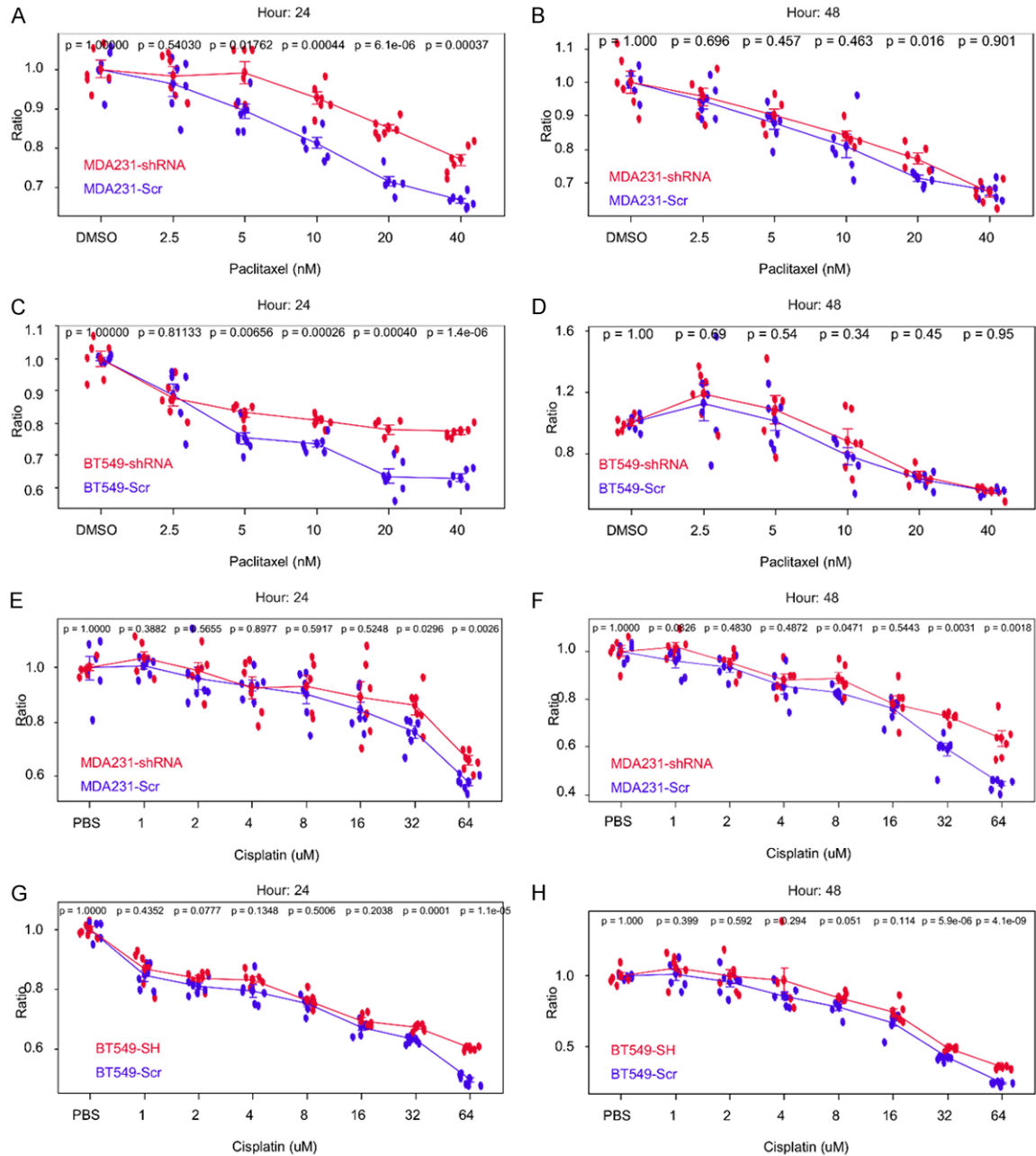


Figure 4. The viability of breast cancer cells treated with chemotherapeutic drugs. Cells were seeded onto 96-well black-well plates with an initial density of 1×10^4 cells/well with six tests per group. Following 24-hour culture and starvation with serum-free medium for 2 hours, cells were then treated with serially diluted doses of cisplatin and paclitaxel as specified. The viability/cytotoxicity of cells was examined using the Alamar Blue assay. A, B. MDA-MB-231 cell lines treated with paclitaxel for 24 and 48 hours, respectively. C, D. BT549 cell lines treated with paclitaxel for 24 and 48 hours, respectively. E, F. MDA-MB-231 cell lines treated with cisplatin for 24 and 48 hours, respectively. G, H. BT549 cell lines treated with cisplatin for 24 and 48 hours, respectively. The comparison of DHX36 shRNA and Scr control was performed using repeated-measures ANOVA. * $P < 0.05$, ** $P < 0.01$.

tumour weight confirmed that the tumours from the DHX36 shRNA group were dramatically heavier than the Scr control ($P < 0.001$, **Figure 5H**). This result, therefore, indicated that knock-

down of DHX36 in MDA-MB-231 cells promoted tumourigenesis, suggesting that DHX36 expression may be crucial for the suppression of neoplastic growth.

DEAH-box nucleic acid helicase DHX36 in breast cancer

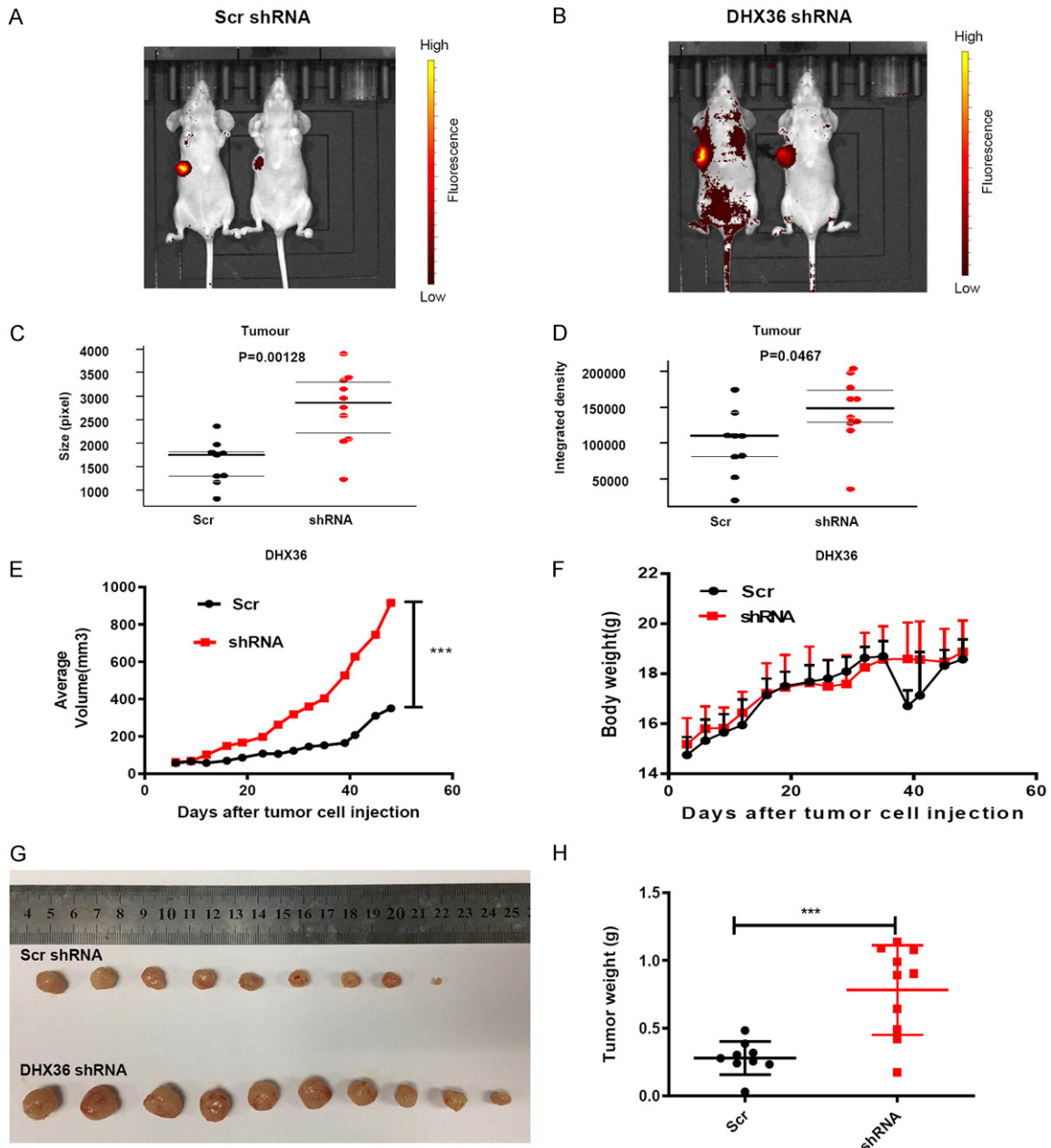


Figure 5. DHX36 knockdown promotes tumor growth in a xenograft mouse model. A, B. Representative *in-vivo* fluorescence images of the breast tumours developed from the mice injected with MDA-MB-231 with Scr control (left) and DHX36 shRNA (right). C. Tumour size estimated using the *in-vivo* images. D. Integrated fluorescence density of the tumours based on the *in-vivo* images. E. Dynamics of the average tumour volume since the injection of tumor cells. F. Dynamics of the bodyweight of the mice since injection. G. The end-point tumours dissected from individual mice (Scr: n=9; DHX36 shRNA: n=10). H. The end-point tumour weight. Quantitative data are presented as mean \pm SEM. *P<0.05, **P<0.01, ***P<0.001.

RNA-Seq transcriptome analysis of stable breast cancer cells indicates that DHX36 is involved in multiple gene regulation pathways

We performed an RNA-Seq transcriptome analysis to examine the gene expression profile

altered by DHX36 shRNA. Overall, following DHX36 knockdown, 2.05% of genes were regulated in BT549 cells, while 1.90% of genes were regulated in MDA-MB-231 cells (**Figure 6A** and **6B**). The top 10 upregulated genes by DHX36 knockdown in both the breast cancer

DEAH-box nucleic acid helicase DHX36 in breast cancer

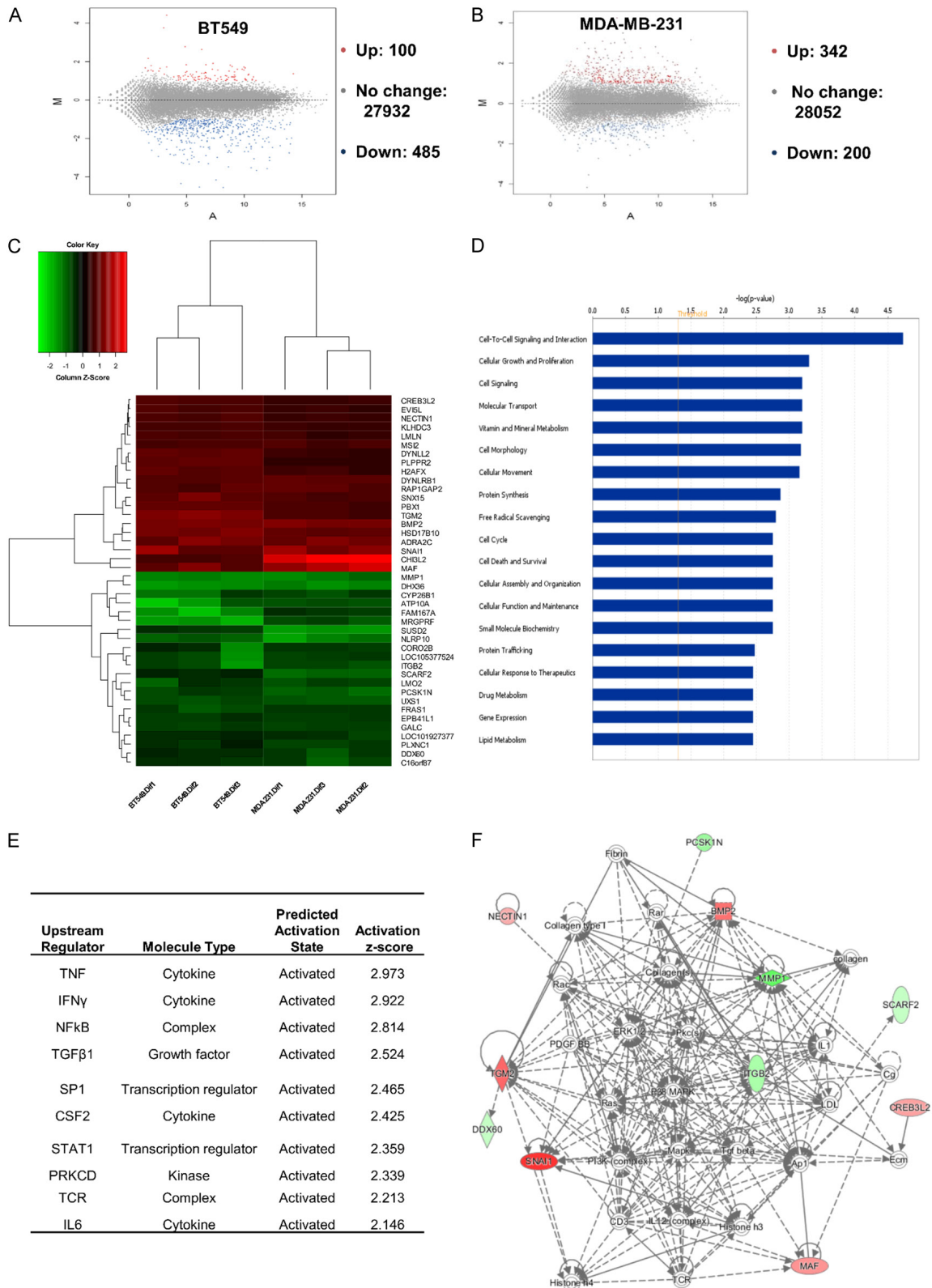


Figure 6. RNA-Seq analysis of the stable breast cancer cells after DHX36 knockdown using shRNA. A, B. MA plot indicating the frequency of the differential gene expression after the stable DHX36 knockdown in BT549 (left) and MDA-MB-231 (right) cells. C. Heatmap of the differential gene expression profile in the two breast cancers with DHX36 shRNA against their Scr control (N=3). D. Cellular functions which were identified to be mediated by the genes regulated by DHX36 KD by gene ontology analysis for RNA-seq. The threshold is P<0.05. E. The predicted upstream regulator of the altered gene profile by the DHX36 knockdown. F. The gene regulation network of the most significantly altered genes by the DHX36 knockdown.

cell lines were CHI3L2, MAF, SNAI1, BMP2, ADRA2C, HSD17B10, TGM2, DYNLRB1, SNX15 and RAP1GAP2. And the top 10 downregulated genes were MMP1, MRGPRF, NLRP10, ATP10A, SUSD2, FAM167A, ITGB2, CYP26B1, UXS1 and PCSK1N (Heatmap showed in **Figure 6C**). As indicated by the gene ontology analysis, DHX36 knockdown altered gene regulation of cell-to-cell signalling and interaction, cellular growth and proliferation, cell signalling and other cellular function (**Figure 6D**). The upstream regulator of these genes could be some cytokines or complex such as TNF, IFN γ and NF κ B, as predicted by using the Ingenuity® Pathway Analysis (IPA) (**Figure 6E**).

DHX36 plays its role in breast cancer cells through stress-associated proteins and mitotic checkpoint protein-serine kinase

We used the Kinex antibody array to determine the molecular signalling mechanisms of DHX36 induced invasion and tumorigenesis in breast cancer cells. As shown in **Figure 7**, two clusters of proteins were identified to be differentially expressed following the DHX36 knockdown. In DHX36 deficient MDA-MB-231 cells, within the cluster of the stress associated kinase proteins, the pan-specific p53, and the phosphorylated p53 protein isoform of S6 were reduced by 47% and 30%, respectively. Within the same cluster, the pan-specific and phosphor (Y913) forms of ROCK1 were also decreased by 34% and 28%, respectively. We also observed the inactivation of the other phosphorylated stress-associated kinase proteins including MYPT1 (T696), MDM2 (S166) and MLC (S19). However, following DHX36 knockdown, the cluster of the Mitotic checkpoint protein-serine kinase proteins was found to be activated. The levels of the phosphorylated proteins of CDK1/2 (T161), CDK1 (T14), CDK1 (T161), CDK1/2 (T14+Y15), CDK1 (T14+Y15) were increased by 133%, 109%, 80%, 60% and 44%, respectively. The original images of the Kinex antibody array analysis were shown in Supporting Information **Figure S5**.

To investigate whether the increase in the CDK levels in the breast cancer cells has an effect on the response susceptibility when CDK is inhibited. We performed proliferation after 48 h treatment with flavopiridol, a CDK inhibitor by ATP competition. The results showed that after

DHX36 knockdown, MDA-MB-231 cells were more sensitive to the inhibitory effect of flavopiridol at different doses including 100 nM (P=0.0087), 200 nM (P=0.0044) and 400 nM (P=0.0022) (Supporting Information **Figure S6A**). BT549 also showed a higher sensitivity following DHX36 knockdown at a dose from 50 nM (P=0.0043) to higher doses including 100 nM (P=0.0022), 200 nM (P=0.0022) and 400 nM (P=0.0022) (Supporting Information **Figure S6B**).

By FACS analysis, we also found that, following the knockdown of DHX36 in BT549 cells, the total and phosphorylated protein levels of JNK were reduced by 36.66% and 35.50%, respectively (**Figure 7C-F**). Similarly, in DHX36-deficient MDA-MB-231 cells, the total and phosphorylated protein levels of JNK were reduced by 20.57% and 16.92%, respectively (**Figure 7G-J**). The reduction of JNK and pJNK in both celllines following the DHX36 knockdown, was confirmed by Western blotting (**Figure 7K**). The qPCR data indicated that the JNK gene expression level was downregulated in cells with the DHX36 shRNA (**Figure 7L**).

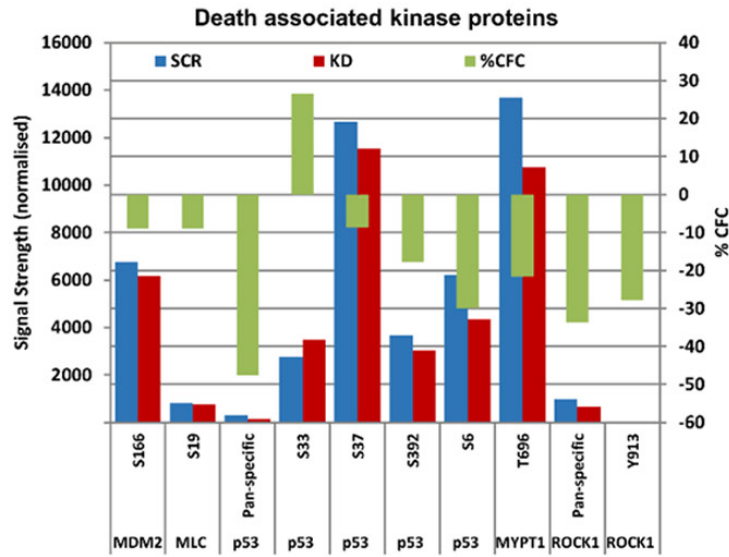
Discussion

There are enormous challenges to elucidate the molecular mechanisms that lead to breast cancer progression and identify new biomarkers for the early detection of this disease [18]. RNA helicases could participate in tumour development and aggression by remodelling complex RNA structures or altering translation of some pro-oncogenic mRNAs [19, 20]. DHX36 is one of the members of the DEAH-box helicases, but its role in breast cancer remains unknown.

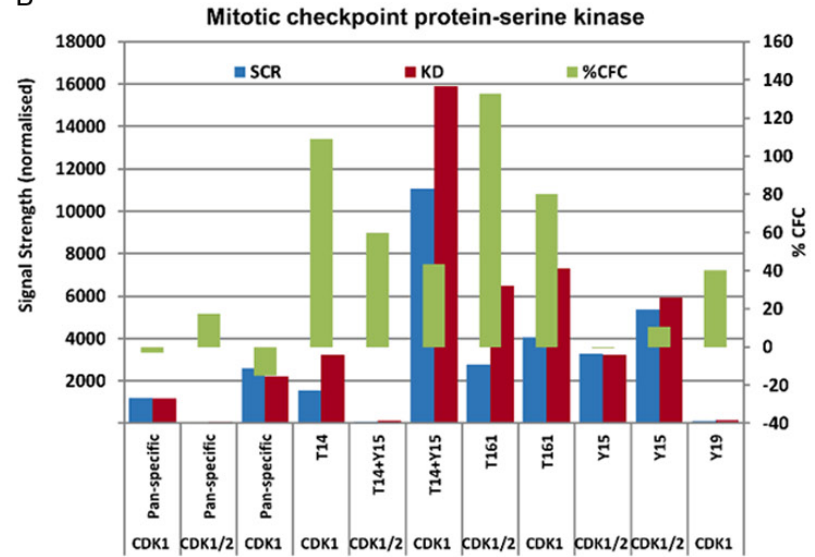
In this study, we identified that DHX36 acts as a prognostic marker in breast cancer. By using the Kaplan Meier survival analysis, we showed that a higher gene expression level of DHX36 is associated with a better OS and RFS in breast cancer patients. Interestingly, the gene expression level of DHX36 in the TNBC is higher than in non-TNBC subtypes. The IHC data indicate that in breast cancer tissues, elevated levels of DHX36 correlate with better overall survival. This is confirmed by the findings in breast cancer tissues, where high levels of DHX36 are associated with a higher stage of the disease.

DEAH-box nucleic acid helicase DHX36 in breast cancer

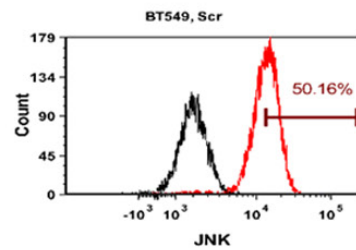
A



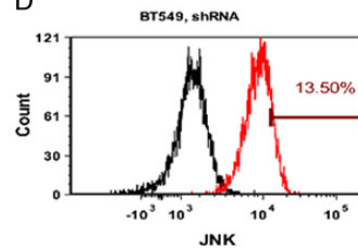
B



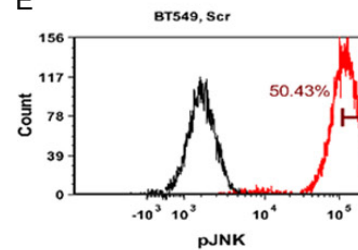
C



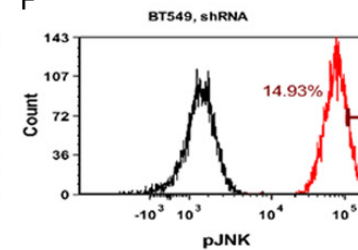
D



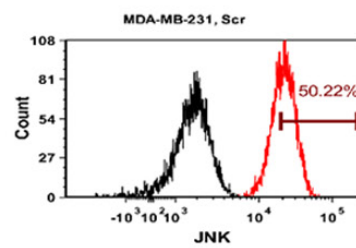
E



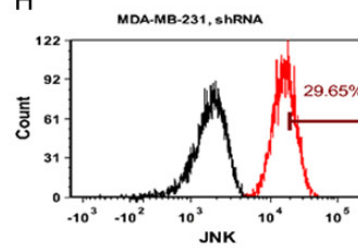
F



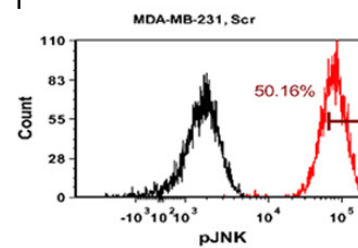
G



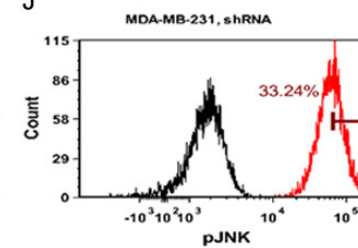
H



I



J



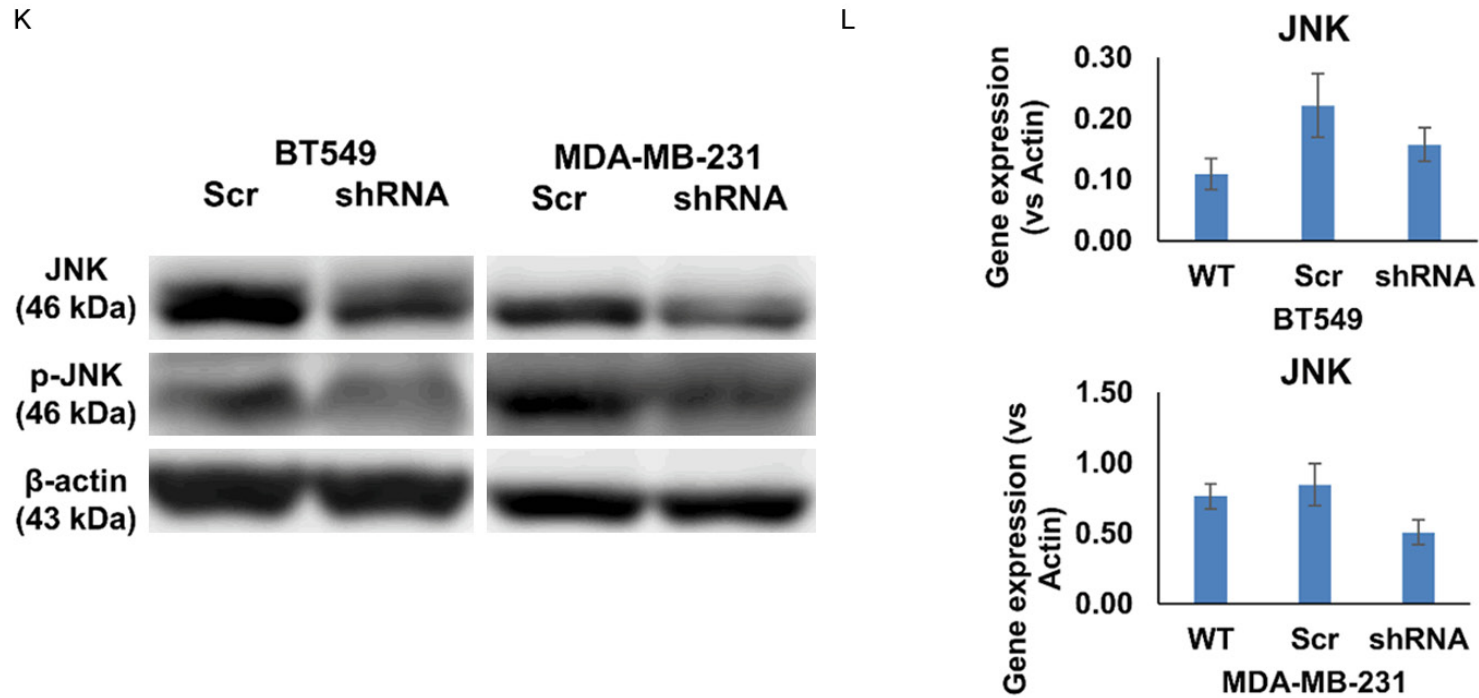


Figure 7. The effect of DHX36 knockdown on signalling pathways of breast cancer cells. A. The profile of stress-associated kinase proteins indicated by the Kinex antibody microarray. B. The profile of mitotic checkpoint protein-serine kinases indicated by the Kinex antibody microarray. The change of protein level in the antibody microarray was calculated as %CFC = $(\text{Signal}_{\text{KD}} - \text{Signal}_{\text{Scr}}) / \text{Signal}_{\text{Scr}} * 100$ after global normalization. FACS analysis was conducted to evaluate the endogenous levels of JNK and phosphor-JNK (pJNK) proteins. C, D. Levels of total JNK protein in the stable BT549 cell lines with Scr control (left) and DHX36 shRNA (right). E, F. Levels of the phosphorylated JNK protein in the stable BT549 cell lines with Scr control (left) and DHX36 shRNA (right). G, H. Levels of total JNK protein in the stable MDA-MB-231 cell lines with Scr control (left) and DHX36 shRNA (right). I, J. Levels of the phosphorylated JNK protein in the stable MDA-MB-231 cell lines with Scr control (left) and DHX36 shRNA (right). K. Western blotting of the JNK and pJNK proteins in the breast cancer cell lines. L. Real-time qRT-PCR showing the gene expression level of JNK in the breast cancer lines.

In addition, the lower staining of DHX36 was observed more frequently in the invasive ductal carcinoma (IDC) than in the invasive lobular carcinoma (ILC) tissues. IDC and ILC are different in multiple clinicopathological features and it is believed that ILC has a favourable response to systemic therapy compared to IDC [21]. However, the pooled analysis using the KM-Plot online database indicates that the DHX36 gene expression level may be positively associated with metastasis and short survival in other solid tumours, such as ovarian and gastric cancer. The contradictory implication of DHX36 in different cancer types may be linked with its functional complexity and heterogeneity of the molecular cancer pathways in which it is involved.

Both *in vitro* and *in vivo* data indicate that DHX36 may inhibit the malignant properties of breast cancer cells. The stable knockdown of DHX36 in TNBC cell lines increased the invasion and decreased the migration properties of the breast cancer cells. The cell cycle analysis suggests that DHX36 deficiency leads to the accumulation of cells in the S-phase of the cell cycle. And the downregulation of DHX36 in breast cancer cells attenuates the apoptosis of breast cancer cells both endogenously and in response to cisplatin. In the presence of DHX36 shRNA, breast cancer cells tend to be more susceptible to the treatments with some chemotherapeutic drugs including cisplatin and paclitaxel in terms of cytotoxicity. Our *in vivo* work demonstrates that the loss of DHX36 function in aggressive MDA-MB-231 cells promotes tumour growth. We, therefore, speculated that the loss of DHX36 drives the cancer progression in breast cancer.

We investigated the role of DHX36 in breast cancer progression through RNA sequencing analysis using DHX36 knockdown cells. The RNA-Seq data indicate that DHX36 is involved in many regulatory network routes through mediating TNF, IFN, NF κ B and TGF β 1. Also, the gene network altered by DHX36 may influence cancer cell behaviour through different pathways, such as cell-to-cell interaction, cell growth, cell signalling, molecular transport and metabolism. It has been shown that DHX36 is involved in TNF α and NF κ B activation in monkey kidney cells in a virus-induced manner [22]. DHX36 can also activate the produc-

tion of IFN β in mouse embryonic fibroblast (MEF) cells or IFN α in dendritic cells by sensing virus stimulation [23, 24]. We therefore speculate that the activation of certain cytokines and growth factors by DHX36 can also occur in breast cancer cells. Besides, the RNA-Seq data suggest that the ITGB2 gene is downregulated, and this may lead to the upregulation of the MMP1 signalling pathway. MMP1 may then downregulate the BMP2 gene, which exerts diverse functions in cancer development and progression [25]. The knockdown of DHX36 also upregulates the gene expression of the SNAIL gene, which is involved in the induction of the epithelial to the mesenchymal transition process.

The high throughput proteomic profile data indicate that, following the knockdown of DHX36 in MDA-MB-231 cells, the level of the death-associated kinase proteins is reduced. In particular, both pan-specific p53 and most of the phosphor-p53 isoforms are decreased in response to the DHX36 knockdown. It is known that almost all eukaryotic mRNAs are subjected to a multi-step pre-mRNA 3'-end processing which is coupled to transcription [26]. DHX36 can specifically bind the p53 RNA G4-forming sequence and therefore maintain p53 pre-mRNA 3'-end processing following UV-induced DNA damage in lung cancer cells [27]. Both MDA-MB-231 and BT549 cell lines have two types of intrinsic p53 mutation, named p53^{280R-K} and p53^{249R-S}, respectively [28]. However, previous studies also suggest that mutant p53 in cancer cells can be either loss-of-function or gain-of-function, and can be stabilized probably through the loss-of-heterozygosity in response to cellular stress [29, 30]. The protein levels of pan-specific and phosphor-ROCK1 are also reduced in DHX36 deficient cells. ROCK1 is an upstream activator of the JNK signalling pathway in cancer [31] and it is involved in actin cytoskeleton destabilisation [32]. As alterations to the actin cytoskeleton can cause changes in various cancer cell properties such as adhesion, migration, invasion, and EMT, we therefore suggest that the reduced level of migration in the breast cancer cells following DHX36 knockdown may be attributed to the decrease of ROCK1.

The protein array data indicate that there is activation by phosphorylation of the mitotic

Breast cancer cell

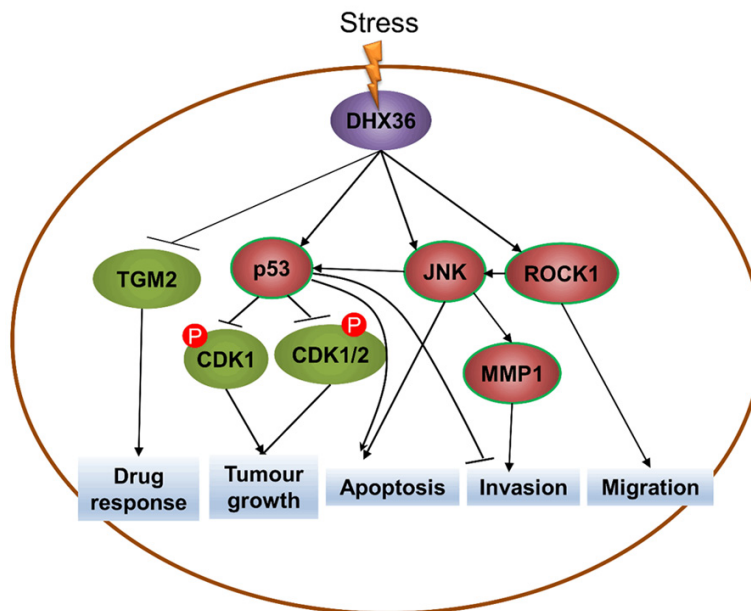


Figure 8. Schematic illustration of molecular mechanisms underlying the tumor suppression mediated by DHX36 in breast cancer cells.

checkpoint protein-serine kinase proteins CDK1 and CDK2. CDK1 is one of the cyclin-dependent kinases (CDKs) which plays a central regulatory role in mitosis initiation and drives cell cycle transition from the G1 phase to the S phase when CDK2 is lost [33]. CDK2 is required for the G1 phase progression and the entry progression into the S phase [34]. In breast cancer, cells with a higher level of CDK2 respond more sensitively to the treatment of paclitaxel [35]. It is known that p53 is an upstream regulator of CDK1 and CDK2 through various downstream effectors such as p21WAF1/CIP1, 14-3-3- σ , reprimin, CD25, cyclin B1 and PLK1 [36].

We also demonstrated that JNK transcription and JNK phosphorylation are reduced following the DHX36 knockdown. The JNK signalling pathway can be activated by some extracellular or intracellular stress such as reactive oxygen species, nitrogen species, UV, inflammation or cytokines [37, 38]. In cancer, activated JNKs can indirectly mediate some aspects of cell behaviour such as growth, transformation and apoptosis by phosphorylating its downstream substrates such as c-Jun, ATF2, ELK1, and p53 [39]. In another way, JNKs may also directly modulate the apoptosis by the phos-

phorylation of the pro- and anti-apoptotic proteins in mitochondria [40].

Chemotherapy resistance remains a major obstacle for the development of an effective breast cancer treatment strategy. It is known that CDK protein kinases may interfere with the DNA repair activity in cancer cells, therefore increasing their sensitivity to certain DNA damaging drugs [41]. We showed that the knockdown of DHX36 appears to sensitize the response of breast cancer cells to some cytotoxic chemotherapeutic drugs such as cisplatin, paclitaxel and flavopiridol, in a dose-dependent manner. This may be due to the elevated levels of certain CDK family members following the DHX-

36 knockdown as described previously (31). Cisplatin, paclitaxel and epirubicin are known as first-line chemotherapeutic drugs. Flavopiridol is a pan-CDK inhibitor which inhibits CDKs by blocking their ATP-binding sites directly. As one of the most investigated CDK inhibitor, flavopiridol has been subjected to considerable clinical trials for its anti-tumour efficacy [42]. Therefore, DHX36 may play a role in modulating the therapeutic response of breast cancer cells although more evidence would be required by further investigation including clinical studies.

Conclusion

In conclusion, to our knowledge, this is the first study that identifies the functional role of DHX36 in breast cancer. Our data indicate that DHX36 acts as a tumour suppressor in human breast cancer. The expression level DHX36 is negatively associated with the survival (OS and RFS) of breast cancer patients. And we believe that the deficiency of DHX36 enhances the invasion property of breast cancer cells and promotes tumour growth by modulating the p53, JNK and ROCK signalling pathways and CDKs (as illustrated in **Figure 8**). Our study therefore unveils the new roles of the

DHX RNA helicase proteins in cancer cells thus potentially opening a new avenue for developing anti-cancer therapeutic strategies with higher efficacy.

Acknowledgements

The authors thank Fiona Ruge and Dr You Zhou for their technical assistance. Dr Jane Lane provided a critical review of the manuscript. This work was financially supported by grants from Cancer Research Wales, Cardiff China Medical Scholarship, Life Sciences Research Network Wales, the National Natural Science Foundation of China (81572596, U1601223, 81502302), and grants from the Guangdong Natural Science Foundation (2017A030313828, 2017A030313489), and funding from the Guangzhou Science and Technology Bureau (201704020131). The authors also gratefully acknowledge financial support from the China Scholarship Council. All animal experiments were performed in accordance with relevant guidelines and regulations approved by the Institutional Animal Care and Use Committee of Sun Yat-sen University Cancer Centre.

Disclosure of conflict of interest

None.

Abbreviations

G4s, guanine-quadruplex structures; DHX36, DEAH-box polypeptide 36; TNBC, triple-negative breast cancer; ER, estrogen receptor; PR, progesterone receptor; HER2, human epidermal growth factor receptor 2; GAPDH, glyceraldehyde-3-phosphate dehydrogenase; IHC, immunohistochemistry; ECIS, electrical cell impedance sensing; IDC, invasive ductal carcinoma; ILC, invasive lobular carcinoma; CDK, cyclin-dependent kinase; RB1, retinoblastoma protein 1; VEGF, vascular endothelial growth factor; HIF1 α , hypoxia-inducible factor 1 α ; PDGFA, platelet-derived growth factor α polypeptide; PDGFR β , PDGF receptor β polypeptide; TERT, human telomerase reverse transcriptase.

Address correspondence to: Yuxin Cui and Wen G Jiang, Cardiff China Medical Research Collaborative, Cardiff University School of Medicine, Heath Park, Cardiff CF14 4XN, UK. E-mail: cuiy7@cardiff.

ac.uk (YXC); jiangw@cardiff.ac.uk (WGJ); Herui Yao, Guangdong Provincial Key Laboratory of Malignant Tumour Epigenetics and Gene Regulation, Sun Yat-sen Memorial Hospital of Sun Yat-sen University, Guangzhou, China. E-mail: yaoherui@mail.sysu.edu.cn

References

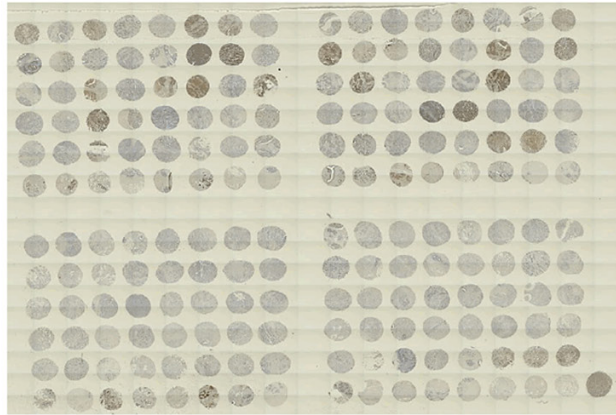
- [1] Torre LA, Bray F, Siegel RL, Ferlay J, Lortet-Tieulent J and Jemal A. Global cancer statistics, 2012. *CA Cancer J Clin* 2015; 65: 87-108.
- [2] Bray F, Ferlay J, Soerjomataram I, Siegel RL, Torre LA and Jemal A. Global cancer statistics 2018: GLOBOCAN estimates of incidence and mortality worldwide for 36 cancers in 185 countries. *CA Cancer J Clin* 2018; 68: 394-424.
- [3] Maizels N. G4-associated human diseases. *EMBO Rep* 2015; 16: 910-922.
- [4] Taunk NK, Goyal S, Wu H, Moran MS, Chen S and Haffty BG. DEAD box 1 (DDX1) expression predicts for local control and overall survival in early stage, node-negative breast cancer. *Cancer* 2012; 118: 888-898.
- [5] Abdel-Fatah TM, McArdle SE, Johnson C, Moseley PM, Ball GR, Pockley AG, Ellis IO, Rees RC and Chan SY. HAGE (DDX43) is a biomarker for poor prognosis and a predictor of chemotherapy response in breast cancer. *Br J Cancer* 2014; 110: 2450-2461.
- [6] Vaughn JP, Creacy SD, Routh ED, Joyner-Butt C, Jenkins GS, Pauli S, Nagamine Y and Akman SA. The DEXH protein product of the DHX36 gene is the major source of tetramolecular quadruplex G4-DNA resolving activity in HeLa cell lysates. *J Biol Chem* 2005; 280: 38117-38120.
- [7] Booy EP, Howard R, Marushchak O, Ariyo EO, Meier M, Novakowski SK, Deo SR, Dzananovic E, Stetefeld J and McKenna SA. The RNA helicase RHAU (DHX36) suppresses expression of the transcription factor PITX1. *Nucleic Acids Res* 2014; 42: 3346-3361.
- [8] Huang W, Smaldino PJ, Zhang Q, Miller LD, Cao P, Stadelman K, Wan M, Giri B, Lei M, Nagamine Y, Vaughn JP, Akman SA and Sui G. Yin Yang 1 contains G-quadruplex structures in its promoter and 5'-UTR and its expression is modulated by G4 resolvase 1. *Nucleic Acids Res* 2012; 40: 1033-1049.
- [9] Luis-Ravelo D, Anton I, Zandueta C, Valencia K, Ormazabal C, Martinez-Canarias S, Guruceaga E, Perurena N, Vicent S, De Las Rivas J and Lecanda F. A gene signature of bone metastatic colonization sensitizes for tumor-induced osteolysis and predicts survival in lung cancer. *Oncogene* 2014; 33: 5090-5099.

- [10] Wan M, Huang W, Kute TE, Miller LD, Zhang Q, Hatcher H, Wang J, Stovall DB, Russell GB, Cao PD, Deng Z, Wang W, Zhang Q, Lei M, Torti SV, Akman SA and Sui G. Yin Yang 1 plays an essential role in breast cancer and negatively regulates p27. *Am J Pathol* 2012; 180: 2120-2133.
- [11] Lee MH, Lahusen T, Wang RH, Xiao C, Xu X, Hwang YS, He WW, Shi Y and Deng CX. Yin Yang 1 positively regulates BRCA1 and inhibits mammary cancer formation. *Oncogene* 2012; 31: 116-127.
- [12] Iwata H, Masuda N, Yamamoto Y, Fujisawa T, Toyama T, Kashiwaba M, Ohtani S, Taira N, Sakai T, Hasegawa Y, Nakamura R, Akabane H, Shibahara Y, Sasano H, Yamaguchi T, Sakamaki K, Bailey H, Cherbavaz DB, Jakubowski DM, Sugiyama N, Chao C and Ohashi Y. Validation of the 21-gene test as a predictor of clinical response to neoadjuvant hormonal therapy for ER+, HER2-negative breast cancer: the TransNEOS study. *Breast Cancer Res Treat* 2019; 173: 123-133.
- [13] Bicker S, Khudayberdiev S, Weiß K, Zocher K, Baumeister S and Schrott G. The DEAH-box helicase DHX36 mediates dendritic localization of the neuronal precursor-microRNA-134. *Genes Dev* 2013; 27: 991-996.
- [14] Shuang T, Wang M, Zhou Y, Shi C and Wang D. NF-kappaB1, c-Rel, and ELK1 inhibit miR-134 expression leading to TAB1 upregulation in paclitaxel-resistant human ovarian cancer. *Oncotarget* 2017; 8: 24853-24868.
- [15] El-Daly SM, Abba ML, Patil N and Allgayer H. miRs-134 and -370 function as tumor suppressors in colorectal cancer by independently suppressing EGFR and PI3K signalling. *Sci Rep* 2016; 6: 24720.
- [16] Matsumura K, Kawasaki Y, Miyamoto M, Kamoshida Y, Nakamura J, Negishi L, Suda S and Akiyama T. The novel G-quadruplex-containing long non-coding RNA GSEC antagonizes DHX36 and modulates colon cancer cell migration. *Oncogene* 2017; 36: 1191-1199.
- [17] Weinreb RN and Lindsey JD. Metalloproteinase gene transcription in human ciliary muscle cells with latanoprost. *Invest Ophthalmol Vis Sci* 2002; 43: 716-722.
- [18] Partridge AH and Carey LA. Unmet needs in clinical research in breast cancer: where do we need to go? *Clin Cancer Res* 2017; 23: 2611-2616.
- [19] Wang Z, Luo Z, Zhou L, Li X, Jiang T and Fu E. DDX5 promotes proliferation and tumorigenesis of non-small-cell lung cancer cells by activating β -catenin signaling pathway. *Cancer Sci* 2015; 106: 1303-1312.
- [20] Yang L, Zhang H, Chen D, Ding P, Yuan Y and Zhang Y. EGFR and Ras regulate DDX59 during lung cancer development. *Gene* 2018; 642: 95-102.
- [21] Barroso-Sousa R and Metzger-Filho O. Differences between invasive lobular and invasive ductal carcinoma of the breast: results and therapeutic implications. *Ther Adv Med Oncol* 2016; 8: 261-266.
- [22] Jing H, Zhou Y, Fang L, Ding Z, Wang D, Ke W, Chen H and Xiao S. DExD/H-box helicase 36 signaling via myeloid differentiation primary response gene 88 contributes to NF- κ B activation to type 2 porcine reproductive and respiratory syndrome virus infection. *Front Immunol* 2017; 8: 1365.
- [23] Yoo JS, Takahashi K, Ng CS, Ouda R, Onomoto K, Yoneyama M, Lai JC, Lattmann S, Nagamine Y and Matsui T. DHX36 enhances RIG-I signaling by facilitating PKR-mediated antiviral stress granule formation. *PLoS Pathog* 2014; 10: e1004012.
- [24] Zhang Z, Kim T, Bao M, Facchinetti V, Jung SY, Ghaffari AA, Qin J, Cheng G and Liu YJ. DDX1, DDX21, and DHX36 helicases form a complex with the adaptor molecule TRIF to sense dsRNA in dendritic cells. *Immunity* 2011; 34: 866-878.
- [25] Vishnubalaji R, Yue S, Alfayez M, Kassem M, Liu FF, Aldahmash A and Alajez NM. Bone morphogenetic protein 2 (BMP2) induces growth suppression and enhances chemosensitivity of human colon cancer cells. *Cancer Cell Int* 2016; 16: 77.
- [26] Wahle E and Rügsegger U. 3'-end processing of pre-mRNA in eukaryotes. *FEMS Microbiol Rev* 1999; 23: 277-295.
- [27] Newman M, Sfaxi R, Saha A, Monchaud D, Teulade-Fichou MP and Vagner S. The G-quadruplex-specific RNA helicase DHX36 regulates p53 Pre-mRNA 3'-end processing following UV-induced DNA Damage. *J Mol Biol* 2017; 429: 3121-3131.
- [28] Lacroix M, Toillon RA and Leclercq G. p53 and breast cancer, an update. *Endocr Relat Cancer* 2006; 13: 293-325.
- [29] Alexandrova EM, Mirza SA, Xu S, Schulz-Hedergott R, Marchenko ND and Moll UM. p53 loss-of-heterozygosity is a necessary prerequisite for mutant p53 stabilization and gain-of-function in vivo. *Cell Death Dis* 2017; 8: e2661.
- [30] Hui L, Zheng Y, Yan Y, Bargonetti J and Foster D. Mutant p53 in MDA-MB-231 breast cancer cells is stabilized by elevated phospholipase D activity and contributes to survival signals generated by phospholipase D. *Oncogene* 2006; 25: 7305.
- [31] Ongusaha PP, Qi HH, Raj L, Kim YB, Aaronson SA, Davis RJ, Shi Y, Liao JK and Lee SW. Identification of ROCK1 as an upstream activator of

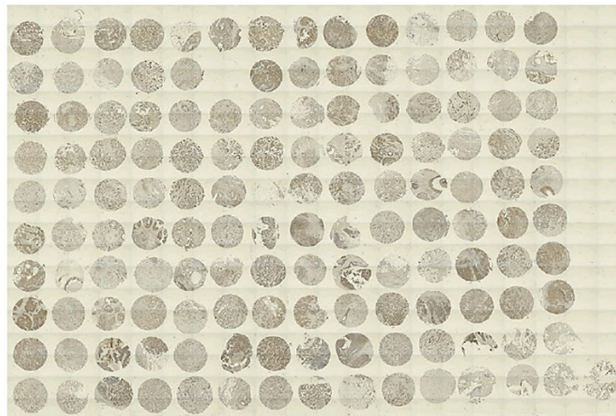
DEAH-box nucleic acid helicase DHX36 in breast cancer

- the JIP-3 to JNK signaling axis in response to UVB damage. *Sci Signal* 2008; 1: ra14.
- [32] Raviraj V, Fok S, Zhao J, Chien HY, Lyons JG, Thompson EW and Soon L. Regulation of ROCK1 via notch1 during breast cancer cell migration into dense matrices. *BMC Cell Biol* 2012; 13: 12.
- [33] Diril MK, Ratnacaram CK, Padmakumar VC, Du T, Wasser M, Coppola V, Tessarollo L and Kaldis P. Cyclin-dependent kinase 1 (Cdk1) is essential for cell division and suppression of DNA re-replication but not for liver regeneration. *Proc Natl Acad Sci U S A* 2012; 109: 3826-3831.
- [34] Bashir T and Pagano M. Cdk1: the dominant sibling of Cdk2. *Nat Cell Biol* 2005; 7: 779-781.
- [35] Nakayama S, Torikoshi Y, Takahashi T, Yoshida T, Sudo T, Matsushima T, Kawasaki Y, Katayama A, Gohda K, Hortobagyi GN, Noguchi S, Sakai T, Ishihara H and Ueno NT. Prediction of paclitaxel sensitivity by CDK1 and CDK2 activity in human breast cancer cells. *Breast Cancer Res* 2009; 11: R12.
- [36] Meek DW. Regulation of the p53 response and its relationship to cancer. *Biochem J* 2015; 469: 325-346.
- [37] Deng T and Karin M. JunB differs from c-Jun in its DNA-binding and dimerization domains, and represses c-Jun by formation of inactive heterodimers. *Genes Dev* 1993; 7: 479-490.
- [38] Shen HM and Liu ZG. JNK signaling pathway is a key modulator in cell death mediated by reactive oxygen and nitrogen species. *Free Radic Biol Med* 2006; 40: 928-939.
- [39] Adler V, Pincus MR, Minamoto T, Fuchs SY, Bluth MJ, Brandt-Rauf PW, Friedman FK, Robinson RC, Chen JM, Wang XW, Harris CC and Ronai Z. Conformation-dependent phosphorylation of p53. *Proc Natl Acad Sci U S A* 1997; 94: 1686-1691.
- [40] Dhanasekaran DN and Reddy EP. JNK signaling in apoptosis. *Oncogene* 2008; 27: 6245.
- [41] Vella S, Tavanti E, Hattinger CM, Fanelli M, Versteeg R, Koster J, Picci P and Serra M. Targeting CDKs with roscovitine increases sensitivity to DNA damaging drugs of human osteosarcoma cells. *PLoS One* 2016; 11: e0166233.
- [42] Robert T, Johnson JL, Guichaoua R, Yaron TM, Bach S, Cantley LC and Colas P. Development of a CDK10/CycM in vitro kinase screening assay and identification of first small-molecule inhibitors. *Front Chem* 2020; 8: 147.

Breast cancer tissue array (#BR1921b)



Breast cancer tissue array (#HBre-Duc140Sur-01)



Breast cancer tissue array (#BR1503e)

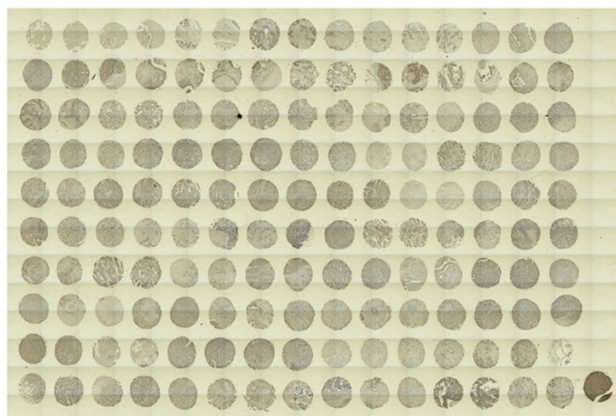


Figure S1. Thumbnail images of the IHC staining of DHX36 in three breast cancer tissue arrays.

DEAH-box nucleic acid helicase DHX36 in breast cancer

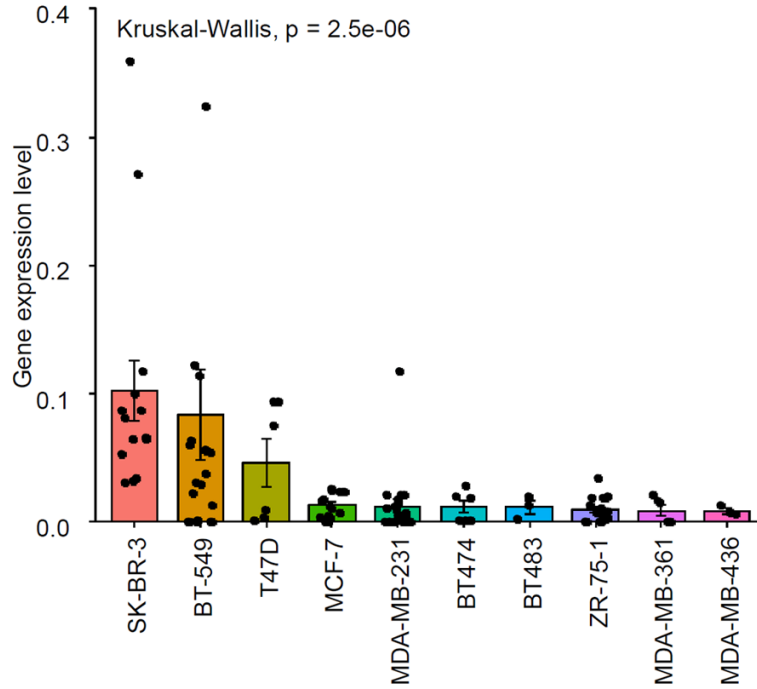


Figure S2. Comparison of DHX36 gene expression in wild-type breast cancer cell lines determined by qRT-PCR and normalized by GAPDH gene expression (fold =1).

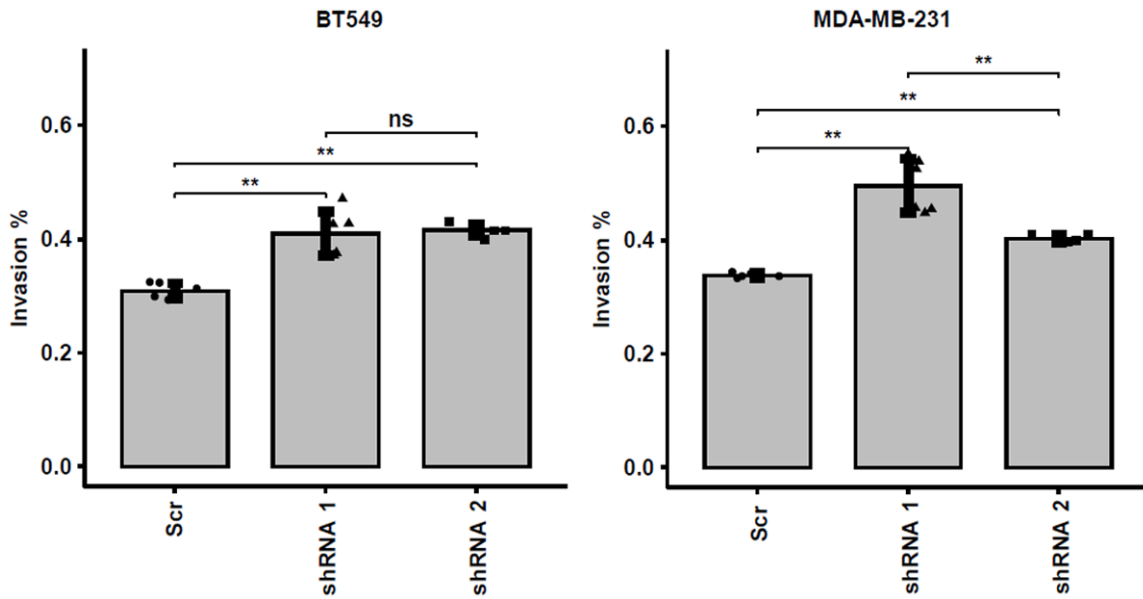


Figure S3. Effect of DHX36 shRNAs on the invasion capacity of stable cell lines. Transwell invasion assay was performed using the stable cell lines derived from BT549 and MDA-MB-231 cells, respectively. Cells invaded through Matrigel-coated membrane inserts (pore size 8 μ m) were stained with Calcein AM and detached using Cell Dissociation Solution, and read using a fluorescence plate reader. Replication points was shown using jitters. ** $P < 0.01$; ns, no statistical significance.

DEAH-box nucleic acid helicase DHX36 in breast cancer

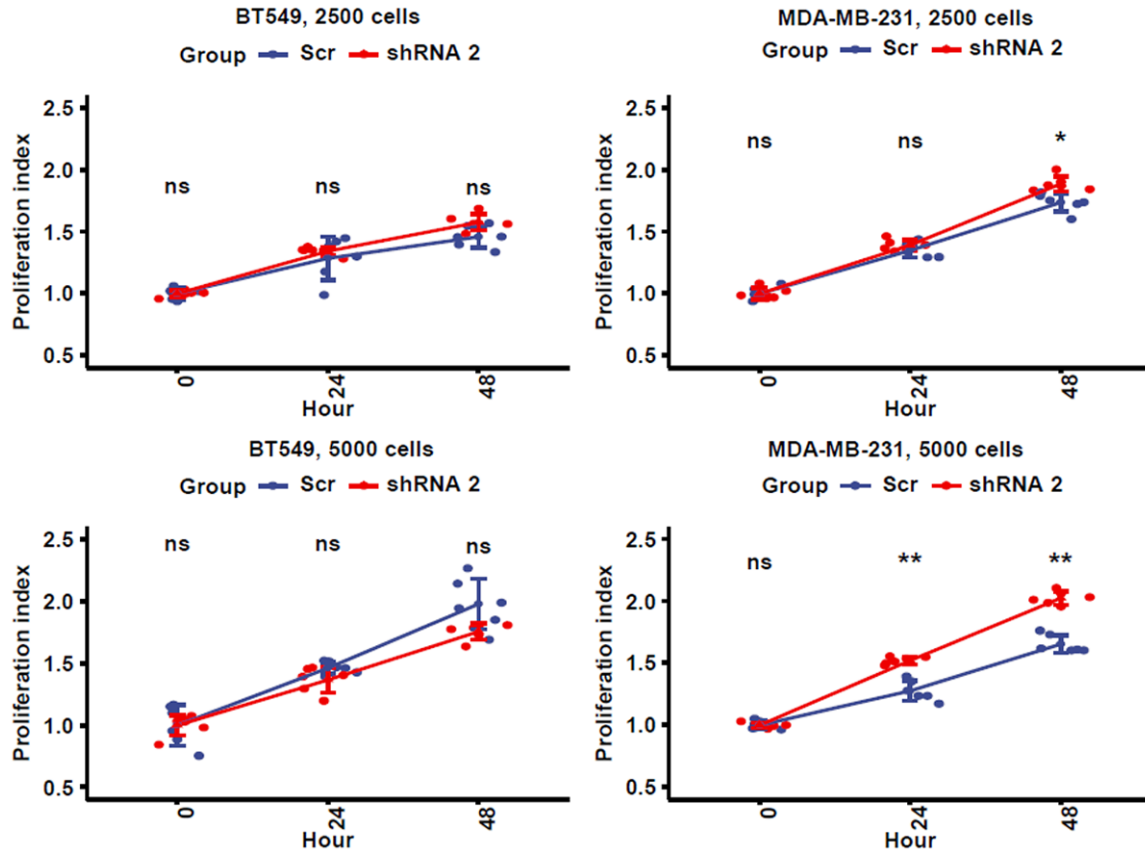


Figure S4. Basal proliferation of the stable breast cancer cell lines. Cells were seeded at densities of 2500 cells/well and 5000 cells/well in 96-well tissue-culture plates. Proliferation measured at the designated time points was normalised with value at Hour 0. The Student's t-test was used to compare the two cell lines (Scr vs. shRNA 2) at each time point. *P<0.05; **P<0.01; ns, no statistical significance.

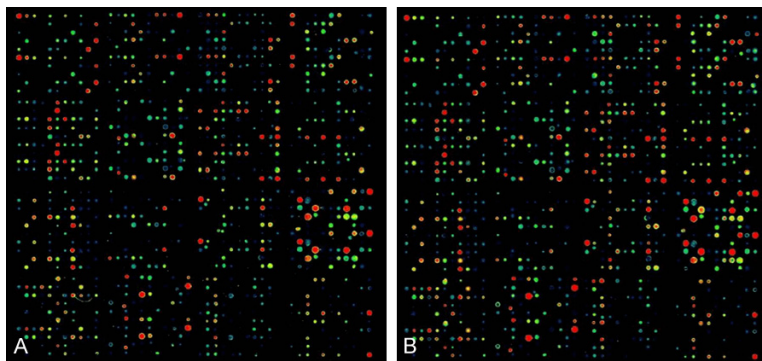


Figure S5. Heatmap images of the Kinex antibody microarray for proteomic analysis in MDA-MB-231 cells. A. Scr control. B. DHX36 shRNA.

DEAH-box nucleic acid helicase DHX36 in breast cancer

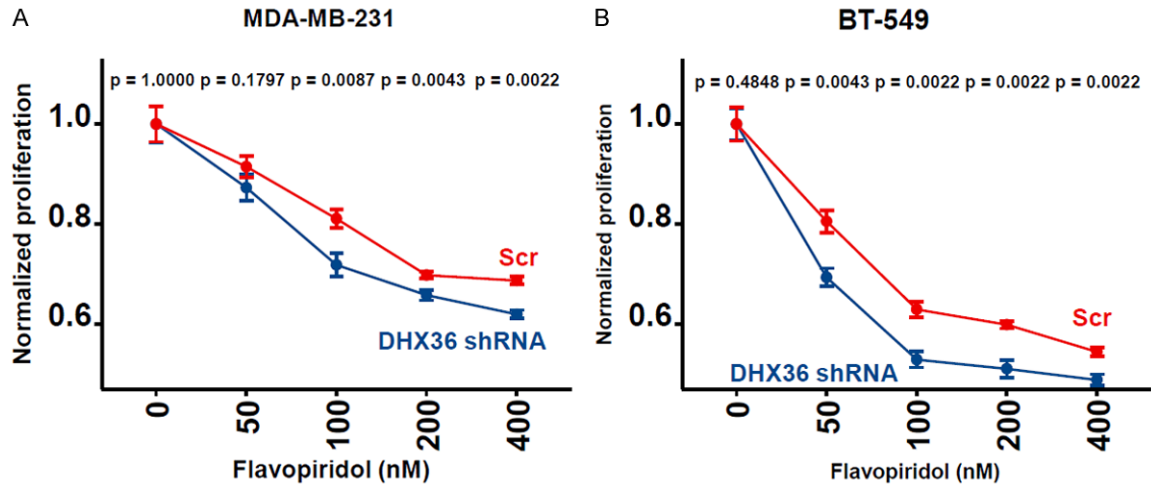


Figure S6. Proliferation of the stable breast cancer cell lines in response to flavopiridol. Cells were seeded onto 96-well black-well plates with an initial density of 1×10^4 cells/well with six tests per group. Following 24-hour culture and starvation with serum-free medium for 2 hours, cells were then treated with serially diluted doses of flavopiridol for 48 hours. The proliferation of cells was examined using the Alamar Blue assay. A. MDA-MB-231 cells. B. BT-549 cells. The Student's t-test was used compare two cell lines for each dose.